Upward Lightning at Wind Turbines: Risk Assessment from Larger-Scale Meteorology

Isabell Stucke[1], Deborah Morgenstern[1], Georg Mayr[1], Thorsten Simon[1], Achim Zeileis[1], Gerhard Diendorfer[2], Wolfgang Schulz[3], and Hannes Pichler[4]

[1]University of Innsbruck
[2]OVE Service GmbH
[3]OVE
[4]OVE, Austria

June 23, 2023

Abstract

Upward lightning (UL) has become a major threat to the growing number of wind turbines producing renewable electricity. It can be much more destructive than downward lightning due to the large charge transfer involved in the discharge process. Ground-truth lightning current measurements indicate that less than 50% of UL could be detected by lightning location systems (LLS). UL is expected to be the dominant lightning type during the cold season. However, current standards for assessing the risk of lightning at wind turbines mainly consider summer lightning, which is derived from LLS. This study assesses the risk of LLS-detectable and LLS-undetectable UL at wind turbines using direct UL measurements at instrumented towers. These are linked to meteorological data using random forests. The meteorological drivers for the absence/occurrence of UL are found from these models. In a second step, the results of the tower-trained models are extended to a larger study area (central and northern Germany). The tower-trained models for LLS-detectable lightning are independently verified at wind turbine sites in this area and found to reliably diagnose this type of UL. Risk maps based on cold season case study events show that high diagnosed probabilities in the study area coincide with actual UL events. This lends credibility to the application of the model to all UL types, increasing both risk and affected areas.

Upward Lightning at Wind Turbines: Risk Assessment from Larger-Scale Meteorology

Isabell Stucke[1,2], Deborah Morgenstern[1,2], Gerhard Diendorfer[3], Georg J. Mayr[2], Hannes Pichler[3], Wolfgang Schulz[3], Thorsten Simon[4], Achim Zeileis[1]

[1]Institute of Statistics, University of Innsbruck, Austria, Innsbruck
[2]Institute of Atmospheric and Cryospheric Sciences, University of Innsbruck, Austria, Innsbruck
[3]OVE Service GmbH, Dept. ALDIS (Austrian Lightning Detection & Information System), Austria, Vienna
[4]Department of Mathematics, University of Innsbruck, Austria, Innsbruck

Key Points:

- Tower-trained random forests can diagnose the risk of upward lightning at wind turbines based on larger-scale meteorological conditions.
- Convective precipitation, larger-scale vertical updraft and the presence of CAPE are most important for upward lightning.
- Slightly elevated terrain and near-coastal conditions tend to increase the risk of upward lightning.

Corresponding author: Isabell Stucke, `isabell.stucke@uibk.ac.at`

Abstract

Upward lightning (UL) has become a major threat to the growing number of wind turbines producing renewable electricity. It can be much more destructive than downward lightning due to the large charge transfer involved in the discharge process. Ground-truth lightning current measurements indicate that less than 50 % of UL could be detected by lightning location systems (LLS). UL is expected to be the dominant lightning type during the cold season. However, current standards for assessing the risk of lightning at wind turbines mainly consider summer lightning, which is derived from LLS. This study assesses the risk of LLS-detectable and LLS-undetectable UL at wind turbines using direct UL measurements at instrumented towers. These are linked to meteorological data using random forests. The meteorological drivers for the absence/occurrence of UL are found from these models. In a second step, the results of the tower-trained models are extended to a larger study area (central and northern Germany). The tower-trained models for LLS-detectable lightning are independently verified at wind turbine sites in this area and found to reliably diagnose this type of UL. Risk maps based on cold season case study events show that high diagnosed probabilities in the study area coincide with actual UL events. This lends credibility to the application of the model to all UL types, increasing both risk and affected areas.

Plain Language Summary

The need to produce renewable energy has recently led to an increase not only in the number of wind turbines, but also in their size. The taller the man-made structure, the greater the likelihood of upward lightning (UL) to initiate from the wind turbine. Each UL event has an initial continuous current, making it ten times longer and much more destructive than a downward lightning event. As UL has become a major weather-related hazard to wind turbines, proper risk assessment has become essential. The problem: Ground-truth current measurements at an instrumented tower in Austria show that less than 50 % of UL is actually detected by lightning location systems (LLS). This study shows that a new approach based on vertically resolved larger-scale meteorology and direct UL measurements from specially instrumented towers, combined with flexible machine learning techniques, succeeds in diagnosing the risk of both LLS-detectable and LLS-undetectable UL at wind turbines in the colder season over a larger study area.

1 Introduction

The growing importance of renewable energy production has recently led to a significant increase in the number of wind turbines (e.g., Pineda et al., 2018). As these structures are typically taller than 100 m, the initiation of upward lightning (UL) propagating from the tall structure towards the clouds is facilitated (Berger, 1967). A tall structure is more likely to experience UL because it is exposed to a stronger electric field compared to the ground. Structures shorter than 100 m mainly experience downward lightning (DL) with leaders propagating from the clouds towards the earth's surface (e.g., Rakov & Uman, 2003).

As wind turbines become taller, UL is the main weather-related cause of severe damage to them (e.g., Rachidi et al., 2008; Montanyà et al., 2016; Pineda et al., 2018; Matsui et al., 2020; Zhang & Zhang, 2020). It can be much more destructive than DL because its initial continuous current (ICC) lasts about ten times longer than the current flow of DL. Ground-truth lightning current measurements on the specially instrumented tower at the top of the Gaisberg mountain (Austria, Salzburg) show that more than 50 % of UL is not detected by conventional lightning location systems (LLS). The reason is that the LLS cannot detect a certain subtype of UL with only an ICC (Diendorfer et al., 2015; March et al., 2016). Although there are towers providing ground-truth lightning current data for LLS-detectable UL (UL-LLS), such as the Säntis Tower in Switzerland, the Gaisberg Tower is the only instrumented tower in Europe providing full information on the occurrence of both UL-LLS and LLS-undetectable UL (UL-noLLS).

Standards for lightning protection of wind turbines (IEC 61400-24, 2019) crucially underestimate the occurrence of UL at wind turbines as they currently rely on only three factors: The height of the wind turbine, the local annual flash density derived from LLS, and an environmental term that includes factors such as terrain complexity or altitude (Rachidi et al., 2008; Pineda et al., 2018; March, 2018; Becerra et al., 2018). Summer lightning activity clearly dominates the annual local flash density due to large amounts of DL caused by deep convection. However, UL is expected to be the dominant lightning type at wind turbines with a tendency to be even more important in the colder season (Diendorfer, 2020; Rachidi et al., 2008). Furthermore, the risk assessment standards cannot take into account UL-noLLS, but only UL-LLS if a tall structure is present.

The main objective of this study is to assess the risk of UL-LLS and UL-noLLS on wind turbines over a larger area. Although LLS are available to analyze UL-LLS at tall structures, direct lightning current measurements show that a significant proportion is missed. Recognizing that conventional LLS cannot assess the full risk of UL at wind turbines, a new approach is used in this study.

It uses machine learning techniques to link the occurrence of UL to the larger-scale meteorological environment. The occurrence of UL can only be provided by ground-truth lightning current measurements. These form the basis for building and training the statistical models that will ultimately be used to assess the risk of UL over an entire study area. Specifically, this study uses conditional inference random forests (Hothorn & Zeileis, 2015), which account for the highly non-linear and complex interactions between the incidence of UL on the tall structures and the atmosphere. Several steps are required to achieve the main goal.

From direct lightning current measurement data at two instrumented towers in Austria (Gaisberg Tower) and Switzerland (Säntis Tower), two models are constructed: One for UL-LLS and one for UL-LLS + UL-noLLS. The aim of these models is, firstly, to determine whether there is a relationship between larger-scale meteorological variables and the occurrence of UL and, secondly, to demonstrate how well larger-scale meteorology can serve as a diagnostic tool for inferring the occurrence of UL.

The advantage of the availability of UL-LLS data helps to verify whether the results from the instrumented towers are transferable. The idea is to extract wind turbine sites within the study area and identify all lightning strikes to them from the colder season (ONDJFMA) using LLS data. Success in reliably diagnosing UL-LLS from larger-scale meteorology in combination with UL ground-truth lightning current measurements provides greater confidence in the results when, in a final step, the risk of UL-noLLS, which cannot be verified using LLS data, is assessed.

The following sections are organized as follows. Section 2 introduces the two instrumented towers that provide the necessary ground-truth data for this study. The first is the Gaisberg Tower, which provides both UL-LLS and UL-noLLS, and the second is the Säntis Tower, which provides only UL-LLS. Furthermore, this section presents the identification of lightning at wind turbines in the study area and the meteorological data used. Section 3 summarizes the procedures and main results from the two instrumented towers. Section 3.1 describes the basic principle of building a random forest model. Section 3.2 presents the performance of the models on the instrumented towers. Furthermore, the most important larger-scale meteorological variables leading to a higher risk of UL are introduced (section 3.3). Then, section 4 presents the results of extending the models from the instrumented towers to the larger study area to find regions with a higher risk of experiencing UL. Section 4.1 diagnoses UL-LLS on wind turbines and presents case studies. Section 4.2 then illustrates and discusses the risk of UL-LLS and UL-LLS

+ UL-noLLS on wind turbines for the entire study period. Section 5 concludes and summarizes the most important findings.

2 Data

This study combines five different data sources: UL data measured directly at the Gaisberg Tower in Austria (Diendorfer et al., 2009) and at the Säntis Tower in Switzerland (Romero et al., 2012); LLS data measured remotely by the European Cooperation for Lightning Detection (EUCLID, Schulz et al., 2016); larger-scale meteorological variables from the reanalysis database ERA5 (Hersbach et al., 2020); wind turbine locations identified using the © OpenStreetMap (OpenStreetMap contributors, 2020) database.

2.1 Direct UL measurements at instrumented towers

Figure 1 shows two of the very few instrumented towers for direct measurement of currents from UL. These are the Gaisberg Tower (1 288 m amsl, 47°48′ N, 13°60′ E) and the Säntis Tower (2 502 m amsl, 47°14′ N, 9°20′ E). Lightning at the instrumented towers is almost exclusively UL. Gaisberg Tower recorded a total of 819 UL events between 2000 and 2015. Säntis Tower recorded 692 UL events between 2010 and 2017.

A sensitive shunt type sensor at Gaisberg allows measurement of all types of upward flashes regardless of the current waveform, that is, UL-LLS and UL-noLLS. However, the inductive sensors used by Säntis cannot measure upward flashes with only an ICC (about 50 %, Diendorfer et al., 2015).

Direct UL current measurements are critical to the construction of the random forest models, which are extended to the larger study area after training on the tower data. The combination of data from both towers provides a sufficiently large dataset and allows the construction of the two types of models to diagnose both UL-LLS and UL-LLS + UL-noLLS.

2.2 UL-LLS at wind turbines and study domain

Remotely detected lightning data from the LLS EUCLID and wind turbine locations derived from © OpenStreetMap serve as verification of the statistical models assessing the risk of UL-LLS for the selected study area.

Within the study area of 50°N–54°N and 6° E–16°E, 27,814 wind turbines have been installed by the end of 2020 (Fig. 1). After extracting the exact locations of these wind turbines, lightning strikes within a 0.003° circular area (approximately within 300 m radius) detected by EUCLID are identified and assumed to be UL. EUCLID measures DL with a high lightning detection efficiency of more than 90 % (Schulz et al., 2016). As mentioned above, UL may be detected less efficiently (< 50 % Diendorfer et al., 2015).

Due to its destructive potential and its severe underestimation in current lightning protection standards, UL, and in particular the risk of UL at wind turbines, shall be explicitly considered in this study. The tower-trained models are based on UL data throughout the year. However, since UL is expected to be dominant in the colder season compared to DL, only the months from October to April, starting from October 2018 to December 2020, are considered in the verification part of the study. Furthermore, since DL is dominant in the warmer season, the extraction of lightning strikes to wind turbines would possibly lead to ambiguity in the identification of DL or UL when considering the whole year.

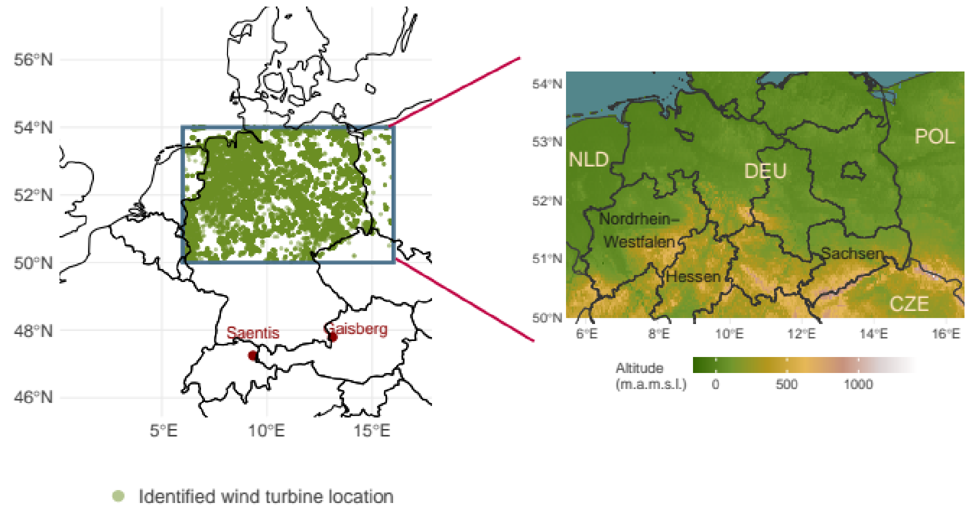

Figure 1. Geographic overview of the instrumented tower locations (Gaisberg and Säntis) as well as the study domain (box). Green dots are manually identified wind turbine locations based on © OpenStreetMap 2020. Right: topographic map of study domain showing altitude above mean sea level. Data taken from Shuttle Radar Topography Mission (Farr & Kobrick, 2000).

2.3 Meteorological data

ERA5 provides an hourly reanalysis of the state of the atmosphere. It has a resolution of 31 km horizontally (grid cell size of 0.25 x 0.25) and 137 levels vertically. This study uses 35 directly available and derived surface, model level, and vertically integrated variables. These reflect variables relevant to cloud electrification, lightning, and thunderstorms (Morgenstern et al., 2022). A complete list of variables can be found in the supporting information file. The data are spatially and temporally bilinearly interpolated to each Gaisberg and Säntis Tower UL observation as well as to each grid cell within the study domain in the verification part of this study.

3 Methodological procedures and findings from the instrumented towers

This section provides the necessary background information on the basic methods as well as important results from the analysis of the instrumented Gaisberg Tower and Säntis Tower. Three different aspects will be covered: First, the principle of how the basic model, a random forest, is constructed and verified. Second, the performance of the models and third, which variables are most important to identify favorable conditions for UL to occur or not.

3.1 Construction and verification of the tower-trained random forests

A machine learning technique that has recently been widely applied in various scientific fields is used to link larger-scale meteorology and the occurrence of UL at the instrumented towers. Random forests Breiman1984 are highly flexible and able to handle nonlinear effects, capturing complex interactions with respect to the stated modeling problem (Strobl et al., 2009).

The occurrence versus non-occurrence of UL is a binary classification problem, which is tackled using 35 larger-scale meteorological variables (predictors). Each meteorological predictor is linked to a situation with or without UL at Gaisberg or Säntis Tower using a random forest. A random forest combines predictions from multiple decision trees trained on randomly selected subsamples of the input data.

Specifically, the trees in the random forest are constructed by capturing the association between the binary response and each of the predictor variables using permutation tests (also known as conditional inference, see Strasser and Weber (1999)). The idea is that at each step in the recursive tree construction, the one predictor variable that has the highest (most significant) association with the response variable is selected. Then, the data set is split with respect to this predictor variable in order to separate the different response classes as well as possible. The splitting is repeated recursively in each of the subsets of the data until some stopping criterion (e.g., regarding significance or subsample size) is met. The forest combines 500 of such trees, where each tree is learned on randomly subsampled two-thirds of the full data set, and only six randomly selected predictors are considered in each split. Finally, the random forest averages the predictions from the ensemble of trees, which stabilizes and improves the prediction performance. See Hothorn et al. (2006) and Hothorn and Zeileis (2015) for more details on the algorithm and implementation.

To validate the resulting models, the input data is split into training and test data samples. The training data is used to train the models, and the unseen test data is used to evaluate the diagnostic capability. Leave-one-out cross-validation is used to validate the models for UL-LLS and UL-LLS + UL-noLLS. The first model for UL-LLS uses both Säntis data and Gaisberg data to increase the size of the training data. The particular flash type that cannot be detected by the Säntis Tower is omitted from the Gaisberg data during training to ensure consistency. The second model for UL-LLS + UL-noLLS uses only Gaisberg data because only the Gaisberg Tower provides complete information on all subtypes of UL.

Between 2000 and 2015, the Gaisberg Tower experienced 247 unique days with UL events. Between 2010 and 2017, the Säntis Tower experienced 186 unique days. Combining the UL days from both towers yields 406 unique days with UL. Each training input data set omits one of the 247 (406) days with UL to use it as test data. This is repeated until each of the 247 (406) days is omitted once for training the random forest models. This results in 247 (406) different models trained on situations with and without UL.

The input model response (that is, did UL occur or not) is sampled so that the two classes are balanced, that is, situations with and without UL are present in equal proportions. To evaluate the performance of the models, the models diagnose the conditional probability on data not considered in the training of the models, that is, on the omitted day. We call the probability conditional because of the balanced model response setup. In order to diagnose the conditional probability of UL also on days without UL, days without UL are randomly sampled from each season between 2000 and 2017. A high diagnostic ability refers to high probabilities when UL occurred at Gaisberg or Säntis in the particular situation (that is, a high true positive rate) and low probabilities when no UL occurred (that is, a low false positive rate).

3.2 Performance of the tower-trained random forests

The tower-trained random forest models can reliably diagnose both UL-LLS and UL-LLS + UL-noLLS when validated on unseen withheld data from the towers. Figure 2 summarizes the cross-validated diagnostic ability according to the random forests for UL-LLS + UL-noLLS (Gaisberg) and UL-LLS (Gaisberg + Säntis). Both model ensembles show similar good diagnostic performance. The diagnosed median conditional prob-

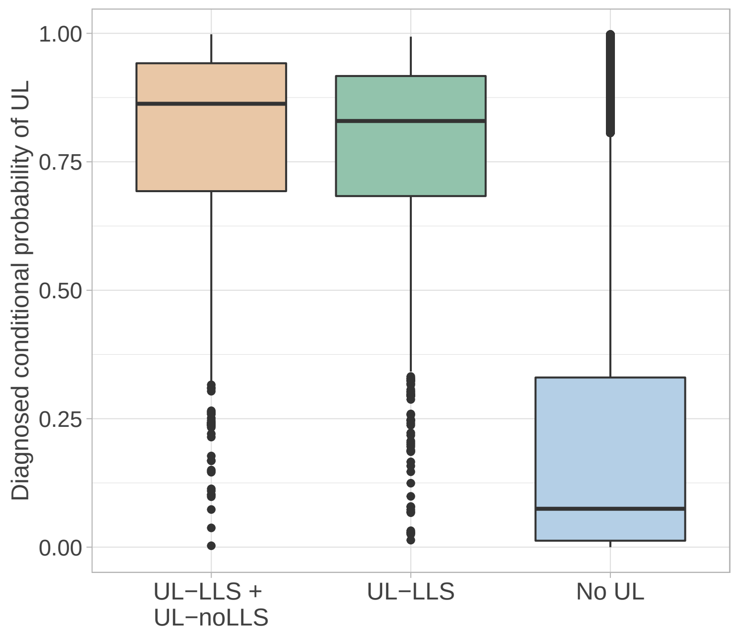

Figure 2. Distributions of diagnosed conditional probabilities in situations with or without UL events. Left: conditional UL probability given that UL was observed in the particular minute (true positive) based on Gaisberg data including all subtypes of UL. Center: conditional UL probability given that UL was observed in the particular minute based on Gaisberg and Säntis data combined. Right: conditional UL probability on randomly sampled days without UL events (false positive).

abilities are about 0.8 that UL was observed in the respective situation (minute). This indicates a high true positive rate. Similarly, for situations without lightning (right), the conditional probabilities are low, indicating a low false positive rate.

The fact that the random forest including UL-noLLS has the highest diagnostic ability shows that the fraction not detected by conventional LLS can indeed be reliably diagnosed by larger-scale meteorology alone. This supports the idea to also investigate the risk of undetectable UL-noLLS and not only UL-LLS.

3.3 Meteorological drivers for UL-LLS at the instrumented towers

Random forests allow to assess the influence of individual variables on the diagnostic performance of the models. This is done by calculating the so-called permutation variable importance. The idea is to break the relationship between the response variable and a predictor variable by neglecting its information when assessing the diagnostic performance of the models. Neglecting the information of a predictor variable is done by permutation, that is, randomly shuffling its values and then assessing how much the diagnostic performance decreases. Figure 3 visualizes the calculated median permutation variable importance according to 100 different random forest models for UL-LLS. Each of the 100 models is based on a balanced proportion of situations with UL and randomly selected situations without UL. The results for the UL-LLS and UL-LLS + UL-noLLS models are very similar.

Convective precipitation has the largest influence on the occurrence of UL according to the random forests based on direct observations from Gaisberg and Säntis Tower (Fig. 3). Neglecting the information of this driver variable reduces the diagnostic performance the most. The second and third most important variables are the maximum updraft velocity and the convective available potential energy (CAPE). A statistical summary of the three most important variables shows that the CAPE at both the Säntis Tower and the Gaisberg Tower is rather low when UL occurs (median value of 68 J kg^{-1}). Convective precipitation comes with a median of 3.8 mm and maximum vertical updraft velocity with a median of $-$ 1.5 m s^{-1}. All values are larger in magnitude than the "average" when looking at every single hour in the time range considered. However, the order of magnitude is not exceptionally high, as can be observed for deep convection, where especially the CAPE values are often higher than 500 J kg^{-1}. An important reason for this may be that at the instrumented towers, UL occurs approximately evenly throughout the year, whereas intense thunderstorms with deep convection and high CAPE values occur mainly in the summer season. Further, this may suggest that the occurrence of UL requires a combination of many different processes that interact to create favorable conditions for UL, which may be even more complex than creating favorable conditions for deep convection.

Other important variables are the maximum precipitation rate, the vertical size of the thundercloud, the amount of ice crystals and solid hydrometeors, and the 2 m dew point temperature.

4 UL at wind turbines

Extraction of wind turbine locations and identification of lightning strikes to them within 300 m in the cold season (ONDJFMA) shows that there are regions within the study area that experience UL more frequently than others (see Fig. 4). Interestingly, the regions that experience UL more frequently (panel (b), dark pink) coincide with regions with many wind turbines. In general, however, it can be observed that regions with a high number of wind turbines (panel (a), dark green) do not necessarily coincide with a high number of ULs, as can be seen for example in the northeastern parts of the study area. The following sections present and discuss the results of extending the results from

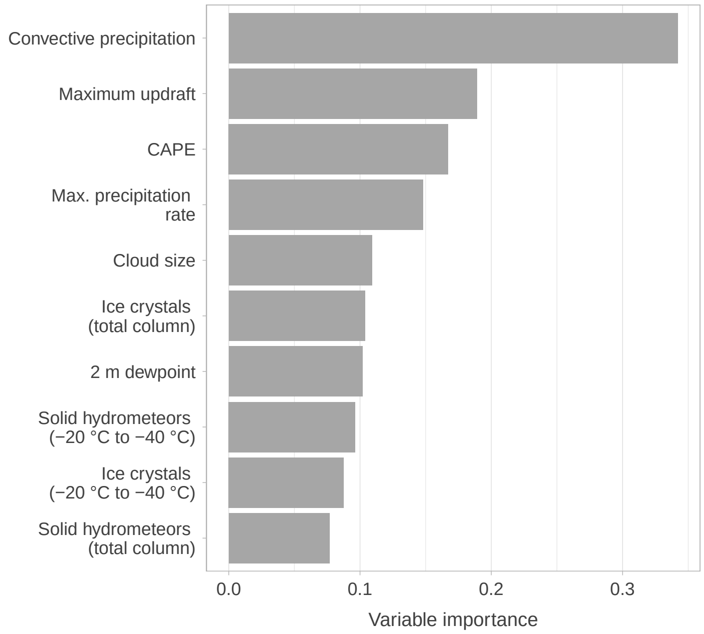

Figure 3. Median permutation variable importance according to 100 different random forests based on balanced proportions of situations with and without UL at the Gaisberg and Säntis Tower.

the instrumented towers to the study area by extracting the locations of wind turbines and analyzing the lightning activity to them.

4.1 Diagnosing UL-LLS at wind turbines from larger-scale meteorological conditions

The random forest models for UL-LLS and UL-LLS + UL-noLLS, based on data from the two instrumented towers, identified larger-scale meteorological variables that are the most important discriminators between situations with and without UL. The tower-trained random forest models are now applied to the larger study area to assess the risk of UL at wind turbines. Lightning measurements from LLS data will verify the results at identified wind turbine sites.

The following results are based on a similar procedure as described in Sect. 3.2, except that each grid cell (31 km x 31 km) of the study domain is used as test data instead of the cross-validated data from the instrumented towers.

To increase the robustness of the results, again 100 different random forest models based on observations from the Gaisberg and the Säntis Tower are used to diagnose the conditional probability of UL on the selected case studies over the study domain. The results in this section visualize the median conditional probabilities diagnosed by the random forest models.

Case studies: UL-LLS at wind turbines

To illustrate the diagnostic ability of the tower-trained random forests for UL-LLS on days with UL events, three different case study days are selected from the colder seasons between 2018 and 2020 in the study area.

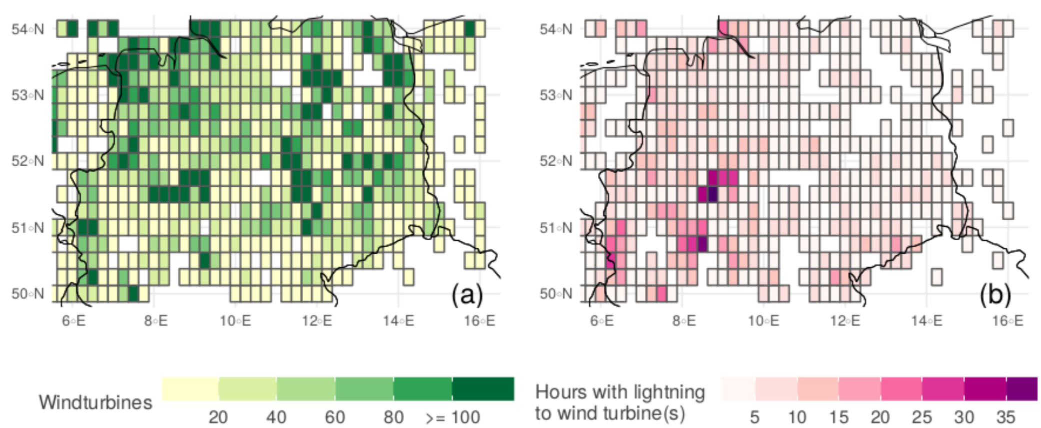

Figure 4. Panel (a): number of wind turbines per grid cell derived from © OpenStreetMap 2020 data. Panel (b): number of hours per grid cell with lightning at wind turbines derived from EUCLID data.

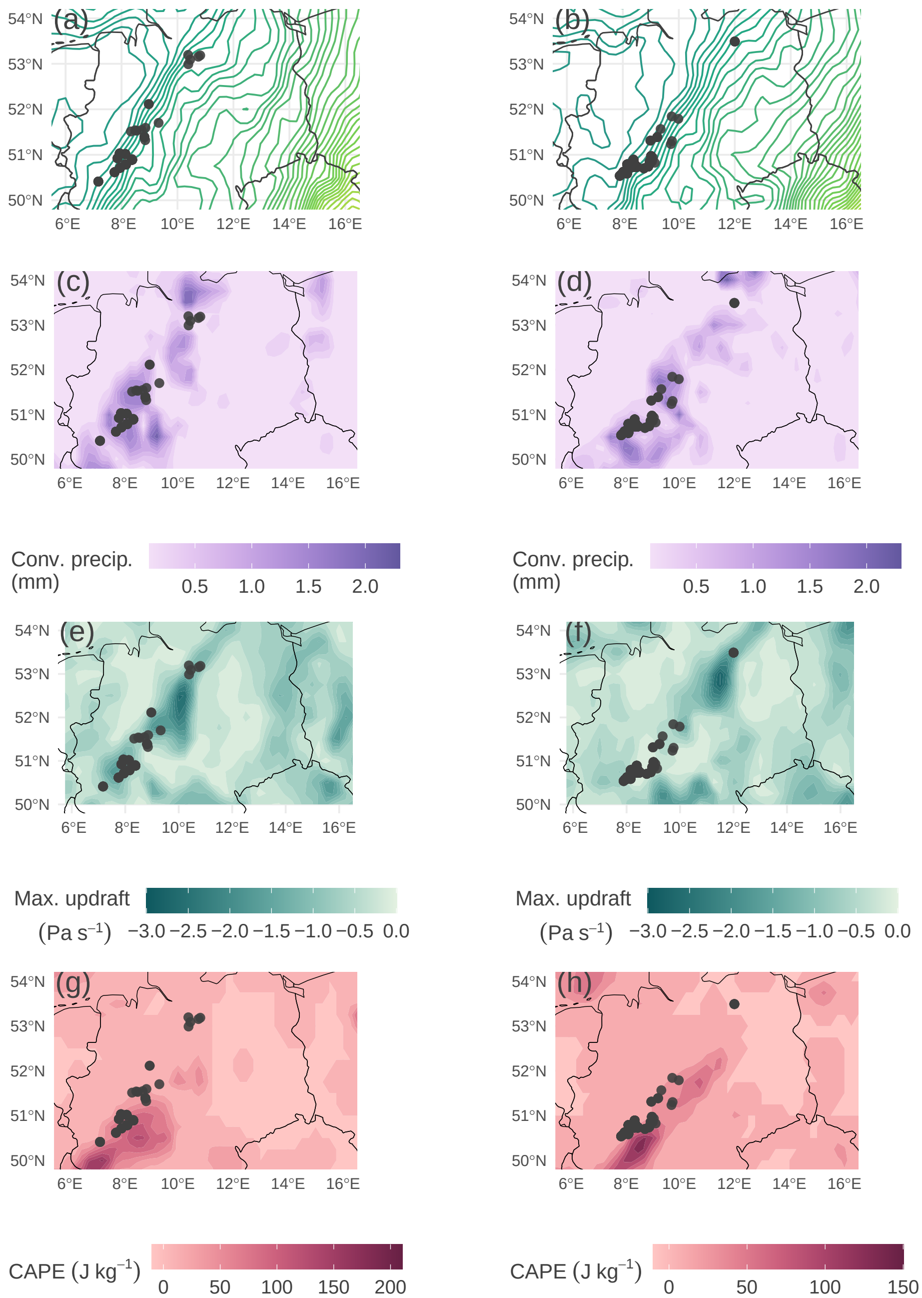

Figure 5. Larger-scale meteorological setting on the 4*th* March 2019 over the study domain. Left column illustrates the setting at 13 UTC, right column at 14 UTC. From upper to lower: spatial distributions of isolines of the 850 hPa temperature (in intervals of 1 K), convective precipitation, the maximum large-scale updraft velocity (negative values is upward motion) and CAPE. Darker colors indicates higher magnitude. Dark gray dots in all figures are flashes within the considered hour and ERA5 grid cell derived from LLS EUCLID data.

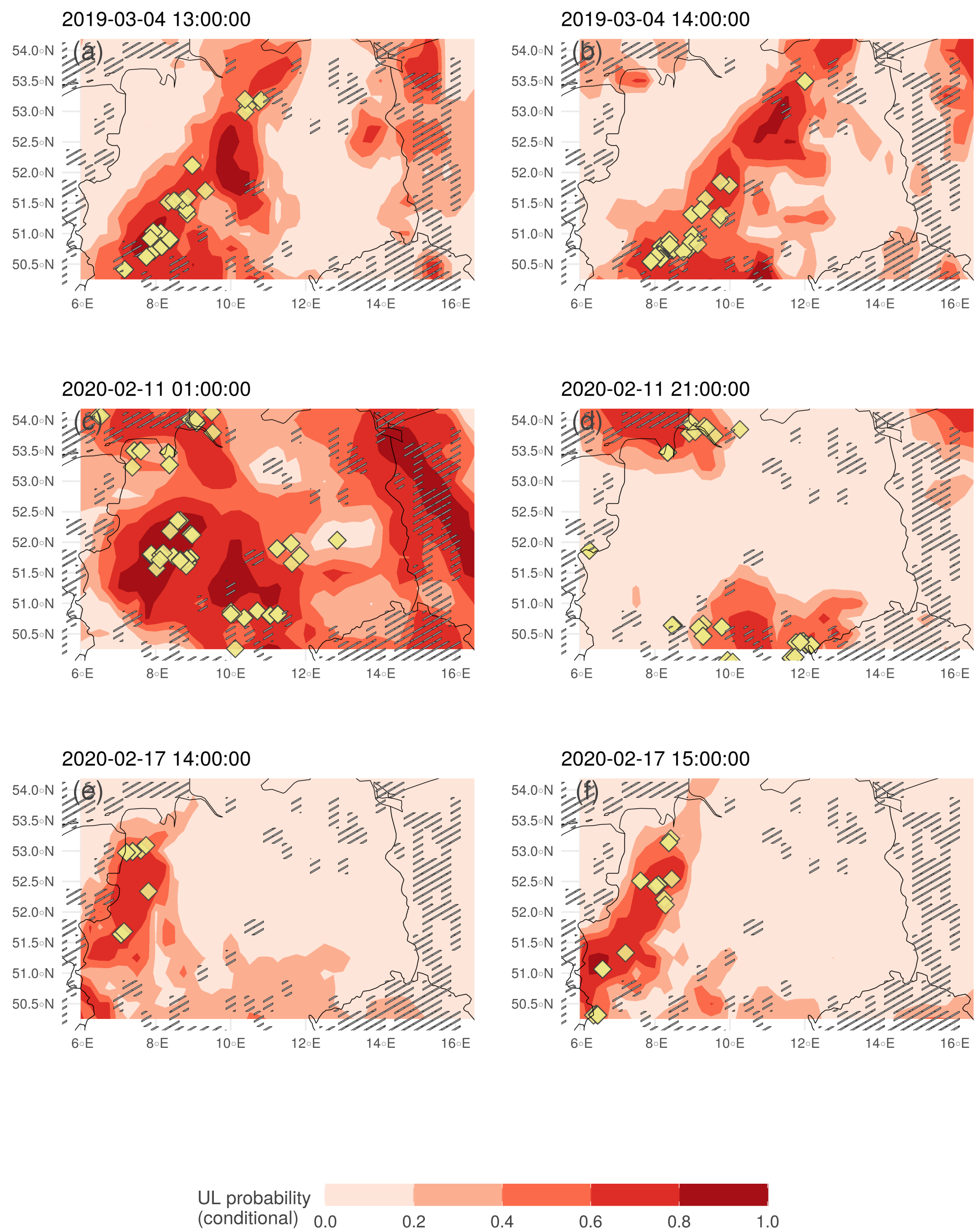

Figure 6. Median diagnosed conditional probability of UL according to 100 random forest models based on Gaisberg and Säntis Tower data (red areas). Yellow symbols are flashes within the considered hour derived from EUCLID data. Gray shaded areas are grid cells without wind turbines.

The selected case study days are characterized by typical weather situations for the colder seasons in the mid-latitudes. The atmosphere in the transitional seasons and in winter tends to be highly variable and influenced by the succession of cyclones and anticyclones that determine the meteorological setting (Perry, 1987). In particular, the development and progression of mid-latitude cyclones provide favorable conditions for so-called wind field thunderstorms (Morgenstern et al., 2022). This type of thunderstorm is associated with, among other things, strong updrafts, high precipitation amounts, and low but present CAPE.

The first case study is considered in more detail with respect to the drivers identified at the instrumented towers (Fig. 3). Figure 5 illustrates the larger-scale isotherm locations, spatial distribution of convective precipitation, maximum updraft velocity, and CAPE on 4 March 2019 at 13 UTC and 14 UTC. LLS detected lightning events at the identified wind turbines within the respective hour are indicated as dark gray dots.

The meteorological setting is determined by the passage of a cold front ahead of a trough around noon. Densely packed isotherms at 850 hPa crossing northern and central Germany from west to east indicate the approximate location of the cold front in panels (a) and (b). The cold front implies locally increased amounts of convective precipitation in (c) and (d), strong updrafts indicated by large negative values in (e) and (f), and slightly increased but generally low CAPE in (g) and (h) compared to deep convection in summer. All three variables show maximally increased values in slightly different areas within the study area induced by the cold front. Convective precipitation shows increased values along the cold front, while the other two variables have locally more concentrated areas with maximum values (e.g. maximum updraft velocity in North/Central Germany).

Figure 6 visualizes the diagnosed conditional probability by the random forest models in red colors for all three case study days. Panels (a) and (b) show the results for the particular case study discussed in Fig. 5. The diagnosed pattern is a result of combining the influence of the three driver variables. This suggests that no single variable can be responsible for the resulting probability map, but rather an interaction of different influencing variables resulting in areas of increased risk of experiencing UL.

The yellow symbols again show lightning strikes over the hour considered. Identified lightning events in yellow require a wind turbine within a maximum distance of 300 m as described in Sect. 2. All other tall structures that may have experienced UL are not considered in this figure. Since the diagnosed probabilities do not depend on wind turbine locations, high probabilities may be diagnosed even though there is no wind turbine installed. Grid cells without wind turbines are shaded gray.

All three case study days in Fig. 6 show that areas with increased diagnosed probability of UL coincide well with identified lightning events in that hour over the study area. In all three case studies, there is a clear separation between areas with very low diagnosed risk and areas with very high diagnosed risk of experiencing UL.

On 11 February 2020, shown in panels (c) and (d) of Fig. 6, the study domain is again in a strong westerly flow associated with locally enhanced convective precipitation, CAPE, and strong updrafts (not shown here). On February 17, 2020, the study area is crossed by a cold front at higher altitudes (above 500 hPa). Despite the different meteorological situation, the conditions are similar to the other case studies, showing elevated values in the three driver variables that strongly influence the diagnosed conditional probability.

4.2 Risk assessment of UL at wind turbines

Identifying areas of increased UL risk due to larger-scale meteorological conditions is a valuable step in assessing the risk of lightning at wind turbines. The case studies clearly show that the observed lightning events at wind turbines coincide with the areas of increased probability diagnosed by the random forest models. The following analysis considers all events within the considered time period in which lightning was detected at wind turbines. Not only the models for UL-LLS shall provide a risk assessment, but now the random forests for UL-LLS + UL-noLLS are additionally applied to the study area and the considered time period.

The considered study period including the transition seasons and winter from 2018 to 2020 counts a total of 185 event days with 1 027 single flash hours and 18 602 single flash events. These numbers are intended as a measure to verify the resulting diagnostic probabilities from the random forest models. Note that these numbers are the lower bound of the number of flashes that actually occurred. Taking into account the uncertainty of manual identification of flashes at wind turbines as well as the uncertainty of UL detection by the LLS, a significantly higher number of actual lightning events at wind turbines can be expected. Furthermore, this verification approach only considers lightning at wind turbines and neglects all other tall structures such as radio towers in the study area that could be affected by UL. In the following, all days within the considered study period are taken as new data for the random forest models to diagnose the conditional probabilities on an hourly basis.

The goal is to identify regions that, according to the random forest models, have a higher risk of UL compared to other regions. This is done by counting the number of hours in each ERA5 grid cell (0.25 x 0.25) that exceed the conditional probability threshold of 0.5.

Risk assessment of UL-LLS at wind turbines

Figure 7a illustrates that there are regions in the study area that have a higher risk of experiencing UL-LLS more frequently than other regions. The western and southwestern parts of the study area have a significantly higher probability of UL-LLS. This is also consistent with panel (b) in Fig. 4, which shows the actually observed hours in which at least one lightning event occurred to a wind turbine within the respective grid cell. Interestingly, areas with higher UL-LLS probabilities in Fig. 7 roughly coincide with regions of elevated topography in the southern third of the domain (cf. Fig. 1). Possible explanations are an increased lightning-effective height (e.g., Shindo, 2018) of the turbines and increased chances for thunderstorm formation due to orographic uplift and thermally induced breezes (Kirshbaum et al., 2018). Sea breezes may also explain the higher probabilities in the northwesternmost, ocean-covered part of the domain.

The successful transfer of the UL-LLS model trained with meteorological data from direct tower measurements to a larger region and its independent verification on wind turbines shows the potential of our approach to produce regionally varying risk maps, which in turn could lead to regionally varying (voluntary or enforced) lightning protection standards for wind turbines.

Risk assessment of UL-LLS + UL-noLLS at wind turbines

The successful transfer of the tower-trained and verified UL-LLS model to a larger domain lends credence to taking the same step with the tower-trained model for all upward lightning (UL-LLS and UL-noLLS), although no data are available for independent verification.

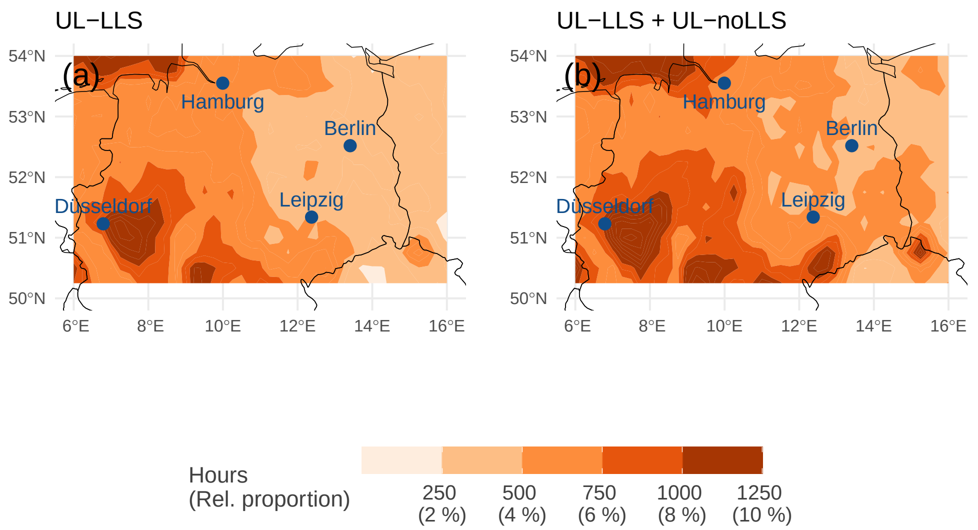

Figure 7. Panels (a) and (b): potential maps for UL in the colder season (ONDJFMA) from 2018 to 2020. Orange colors are median of hours per grid cell exceeding conditional probabilities of 0.5 according to 100 random forest models. Panel (a) shows results according to models based on Gaisberg and Säntis data combined. Panel (b) shows results according to models based on Gaisberg data also including the UL-noLLS. Relative proportion of in total 12480 hours are given as reference.

Panel (b) in Fig. 7 shows that more flashes are expected when the LLS-undetectable UL flash type is added. The pattern of areas with increased risk of experiencing UL is similar, although some of the more frequently affected areas are enlarged. This suggests that there are similar mechanisms resulting from larger-scale meteorology that lead to the UL-LLS or UL-noLLS flash types. The risk is most pronounced in regions with elevated topography in the southern part of the domain and in the northwesternmost coastal region.

5 Conclusions

Upward (UL) lightning that strikes tall structures such as wind turbines is much more destructive than downward (DL) lightning. Each UL flash begins with an initial continuous current (ICC) that lasts about ten times longer than DL, transferring much more charge to the tall structure. Furthermore, direct measurements of upward lightning suggest that less than 50 % of UL events can be detected by most lightning location systems (LLS) because they are unable to detect UL with only an ICC.

Current lightning protection standards are based on the annual flash density derived from LLS data, which is clearly dominated by DL in the warm season. UL that is not detectable by LLS (UL-noLLS) is completely neglected and UL in the cold season is severely underestimated. The basic knowledge about the occurrence of UL is still incomplete, which hinders a proper risk assessment of UL at wind turbines.

The lack of consideration of UL-noLLS and the importance of the cold season for UL will therefore significantly underestimate the risk of UL to wind turbines. This study uses rare direct UL measurements with larger-scale meteorological data in a machine learning model to estimate the risk of all UL, including UL-noLLS, on wind turbines.

This study's first step is to train and validate two different random forest models based on long-term observations from two specially instrumented towers. One model considers only LLS-detectable UL (UL-LLS) and one model considers UL-LLS + UL-noLLS. The model input data are direct UL measurements from the Gaisberg Tower (Austria, 2000-2015) and the Säntis Tower (Switzerland, 2010-2017). While the sensor at the Gaisberg Tower also measures UL-noLLS, the sensor at the Säntis Tower misses most of them.

In a second step, the random forest models are extended to a larger study area (50°N–54°N and 6° E–16°E) to identify areas with increased risk of UL in the colder season (OND-JFMA). As a verification, all lightning strikes from LLS data on wind turbines extracted from © OpenStreetMap data are compared to the diagnosed probabilities by the random forests.

The results show that UL can be reliably diagnosed by the tower-trained random forest models at the Gaisberg and Säntis towers. The larger-scale meteorological drivers are large amounts of (convective) precipitation, strong vertical updraft velocities, and slightly elevated CAPE. Furthermore, the vertical extent of the clouds and the amount of ice crystals and solid hydrometeors are important variables.

Extending the random forests to a larger domain shows that the probability maps match the observed lightning strikes at wind turbines. The extension of the models trained at the Gaisberg Tower to include UL-noLLS flashes shows that areas with an increased risk of experiencing UL are expected to experience UL even more frequently. The western and southern part of the domain in northwestern Germany with elevated topography and the coastal region in the northwesternmost part are most at risk for UL at wind turbines.

This study demonstrates that direct UL measurements at an instrumented tower can be reliably modeled from larger-scale meteorological conditions in a machine learning model (random forest). The study also proposes a novel way to justify the transfer of this model to a larger region using UL-LLS data at wind turbine sites. As a result, regionally detailed risk maps of UL at wind turbines can be produced.

Open Research

Data availability

ERA5 data are freely available at the Copernicus Climate Change Service (C3S) Climate Data Store Hersbach et al. (2020). The results contain modified Copernicus Climate Change Service information (2020). Neither the European Commission nor ECMWF is responsible any use that may be made of the Copernicus information or data it contains. EUCLID data and ground truth lightning current measurements from the Gaisberg Tower are available only on request. For more details contact Wolfgang Schulz or Siemens BLIDS.

Software

All calculations as well as setting up the final data sets, modeling and the diagnosis were performed using R R Core Team (2021), using packages netCDF4 Pierce (2019), partykit Hothorn and Zeileis (2015), ggplot2 package Wickham (2016). Retrieving the raw data and deriving further variables from ERA5 required using Python3 Van Rossum and Drake (2009) and cdo Schulzweida (2019).

Competing interests

The authors declare that they have no conflict of interest.

Acknowledgements

We acknowledge the funding of this work by the Austrian Research Promotion Agency (FFG), project no. 872656 and Austrian Science Fund (FWF) grant no. P 31836. We thank the EMC Group of the Swiss Federal Institute of Technology (EPFL) for providing the data of the Säntis Tower strikes.

Provided Author contributions

Isabell Stucke: Conceptualization, Data Curation, Formal Analysis, Investigation, Methodology, Validation, Software, Visualization, Writing – Original Draft, Writing – Review Editing, Deborah Morgenstern: Conceptualization, Data Curation, Writing – Review Editing, Gerhard Diendorfer: Conceptualization, Funding Acquisition, Resources, Writing – Review Editing, Georg J. Mayr: Conceptualization, Funding Acquisition, Project Administration, Supervision, Writing – Review Editing , Hannes Pichler: Conceptualization, Funding Acquisition, Resources, Wolfgang Schulz: Conceptualization, Funding Acquisition, Resources, Writing – Review Editing , Thorsten Simon: Conceptualization, Data Curation, Formal Analysis, Supervision, Writing – Review Editing , Achim Zeileis: Formal Analysis, Methodology, Project Administration, Software, Supervision, Writing – Review Editing

References

Becerra, M., Long, M., Schulz, W., & Thottappillil, R. (2018). On the estimation of the lightning incidence to offshore wind farms. *Electric Power Systems Research*, *157*, 211–226. Retrieved from `https://www.sciencedirect.com/science/article/pii/S0378779617304790` (accessed 2022-12-22) doi: 10.1016/j.epsr.2017.12.008

Berger, K. (1967). Novel observations on lightning discharges: Results of research on mount san salvatore. *Journal of the Franklin Institute*, *283*(6), 478–525. Retrieved from `https://www.sciencedirect.com/science/article/pii/0016003267905984` (accessed 2023-03-08) doi: 10.1016/0016-0032(67)90598-4

Diendorfer, G. (2020). *Probability of lightning strikes to wind turbines in europe during winter months* (Tech. Rep.). Copernicus Meetings. doi: 10.5194/egusphere-egu2020-3337

Diendorfer, G., Pichler, H., & Mair, M. (2009). Some parameters of negative upward-initiated lightning to the gaisberg tower (2000–2007). *IEEE Transactions on Electromagnetic Compatibility*, *51*(3), 443–452. Retrieved from `https://ieeexplore.ieee.org/document/5089467` (accessed 2021-05-24) doi: 10.1109/TEMC.2009.2021616

Diendorfer, G., Pichler, H., & Schulz, W. (2015). LLS detection of upward initiated lightning flashes. In *Proc. 9th asia-pacific international conference on lightning (APL)* (p. 5). Nagoya, Japan. Retrieved from `https://www.ove.at/fileadmin/user_upload/aldis/publication/2015/2_APL2015_Diendorfer.pdf` (accessed 2021-06-17)

Farr, T. G., & Kobrick, M. (2000). Shuttle radar topography mission produces a wealth of data. *Eos, Transactions American Geophysical Union*, *81*(48), 583–585.

Hersbach, H., Bell, B., Berrisford, P., Hirahara, S., Horányi, A., Muñoz-Sabater, J., … Thépaut, J.-N. (2020). The ERA5 global reanalysis. *Quarterly Journal of the Royal Meteorological Society*, *146*(730), 1999–2049. Retrieved from `https://rmets.onlinelibrary.wiley.com/doi/abs/10.1002/qj.3803` (accessed 2021-04-12) doi: 10.1002/qj.3803

Hothorn, T., Hornik, K., & Zeileis, A. (2006). Unbiased recursive partitioning: A conditional inference framework. *Journal of Computational and Graphical Statistics*, *15*(3), 651–674. (accessed 2022-04-27) doi: 10.1198/106186006X133933

Hothorn, T., & Zeileis, A. (2015). partykit: A modular toolkit for recursive partytioning in R. *Journal of Machine Learning Research*, *16*(118), 63905–3909. Retrieved from `http://jmlr.org/papers/v16/hothorn15a.html` (accessed 2022-04-27)

IEC 61400-24. (2019). *International standard: Wind energy generation systems - part 24: Lightning protection* (Second ed.). Geneva, Switzerland: International Electrotechnical Commission (IEC).

Kirshbaum, D., Adler, B., Kalthoff, N., Barthlott, C., & Serafin, S. (2018). Moist orographic convection: Physical mechanisms and links to surface-exchange processes. *Atmosphere*, *9*(3), 80. doi: 10.3390/atmos9030080

March, V. (2018). Key issues to define a method of lightning risk assessment for wind farms. *Electric Power Systems Research*, *159*, 50-57. Retrieved from `https://www.sciencedirect.com/science/article/pii/S0378779617303450` (Recent Developments on Lightning Research and Protection Technologies) doi: 10.1016/j.epsr.2017.08.020

March, V., Montanyà, J., Fabró, F., van der Velde Oscar, Romero, D., Solà, G., … Pineda, N. (2016). Winter lightning activity in specific global regions and implications to wind turbines and tall structures. In *2016 33rd international conference on lightning protection (ICLP), 25–30 september 2016, estoril, portugal.* (accessed 2022-04-09) doi: 10.1109/ICLP.2016.7791447

Matsui, M., Michishita, K., & Yokoyama, S. (2020). Cloud-to-ground lightning flash density and the number of lightning flashes hitting wind turbines in japan. *Electric Power Systems Research*, *181*, 106066. Retrieved from `https://www.sciencedirect.com/science/article/pii/S0378779619303852?via\%3Dihub` (accessed 2021-03-24) doi: 10.1016/j.epsr.2019.106066

Montanyà, J., Fabró, F., van der Velde, O., March, V., Williams, E. R., Pineda, N., … Freijo, M. (2016). Global distribution of winter lightning: A threat to wind turbines and aircraft. *Natural Hazards and Earth System Sciences*, *16*(6), 1465–1472. Retrieved from `https://www.nat-hazards-earth-syst-sci.net/`

16/1465/2016/nhess-16-1465-2016.pdf (accessed 2020-02-19) doi: 10.5194/nhess-16-1465-2016

Morgenstern, D., Stucke, I., Simon, T., Mayr, G. J., & Zeileis, A. (2022). Differentiating lightning in winter and summer with characteristics of the wind field and mass field. *Weather and Climate Dynamics*, *3*(1), 361–375. Retrieved from https://wcd.copernicus.org/articles/3/361/2022/ (accessed 2022-04-07) doi: 10.5194/wcd-3-361-2022

OpenStreetMap contributors. (2020). *Planet dump retrieved from https://planet.osm.org* . https://www.openstreetmap.org.

Perry, A. (1987). Middle latitude climates. In *Climatology* (pp. 581–583). Boston, MA: Springer US. doi: 10.1007/0-387-30749-4_116

Pierce, D. (2019). ncdf4: Interface to unidata netCDF (version 4 or earlier) format data files [Computer software manual]. Retrieved from https://CRAN.R-project.org/package=ncdf4 (R package version 1.17)

Pineda, N., Montanyà, J., Salvador, A., van der Velde, O. A., & López, J. A. (2018). Thunderstorm characteristics favouring downward and upward lightning to wind turbines. *Atmospheric Research*, *214*, 46-63. doi: https://doi.org/10.1016/j.atmosres.2018.07.012

R Core Team. (2021). R: A language and environment for statistical computing [Computer software manual]. Vienna, Austria. Retrieved from https://www.R-project.org/

Rachidi, F., Rubinstein, M., Montanyà, J., Bermudez, J.-L., Sola, R. R., Solà, G., & Korovkin, N. (2008). A review of current issues in lightning protection of new-generation wind-turbine blades. *IEEE Transactions on Industrial Electronics*, *55*(6), 2489–2496. (accessed 2022-04-27) doi: 10.1109/TIE.2007.896443

Rakov, V. A., & Uman, M. A. (2003). *Lightning: Physics and effects*. Cambridge University Press. doi: 10.1017/CBO9781107340886

Romero, C., Paolone, M., Rubinstein, M., Rachidi, F., Rubinstein, A., Diendorfer, G., . . . Zweiacker, P. (2012). A system for the measurements of lightning currents at the säntis tower. *Electric Power Systems Research*, *82*(1), 34–43. (accessed 2022-04-27) doi: https://doi.org/10.1016/j.epsr.2011.08.011

Schulz, W., Diendorfer, G., Pedeboy, S., & Poelman, D. R. (2016). The european lightning location system EUCLID - part 1: Performance analysis and validation. *Natural Hazards and Earth System Sciences*, *16*(2), 595–605. Retrieved from https://pdfs.semanticscholar.org/dba9/b99d6050e3032b823dc88302fd922b89ab83.pdf (accessed 2020-02-19) doi: 10.5194/nhess-16-595-2016

Schulzweida, U. (2019). *CDO user guide*. doi: 10.5281/zenodo.3539275

Shindo, T. (2018). Lightning striking characteristics to tall structures. *IEEJ Transactions on Electrical and Electronic Engineering*, *13*(7), 938–947. doi: 10.1002/tee.22649

Strasser, H., & Weber, C. (1999). *On the asymptotic theory of permutation statistics* (Report Series SFB "Adaptive Information Systems and Modelling in Economics and Management Science" No. 27). SFB Adaptive Information Systems and Modelling in Economics and Management Science, WU Vienna University of Economics and Business. Retrieved from https://epub.wu.ac.at/102/ (accessed 2023-03-29)

Strobl, C., Malley, J., & Tutz, G. (2009). An introduction to recursive partitioning: Rationale, application, and characteristics of classification and regression trees, bagging, and random forests. *Psychological Methods*, *14*(4), 323–348. (accessed 2022-04-27) doi: 10.1037/a0016973

Van Rossum, G., & Drake, F. L. (2009). *Python 3 reference manual*. Scotts Valley, CA: CreateSpace Independent Publishing Platform. (accessed 2021-03-09)

Wickham, H. (2016). *ggplot2: Elegant graphics for data analysis*. Springer Verlag New York. Retrieved from https://ggplot2.tidyverse.org

Zhang, Y., & Zhang, X. (2020). Statistic analysis of lightning transients on wind turbines. *Journal of Renewable and Sustainable Energy*, *12*(6), 063302. doi: 10.1063/5.0031506

Upward Lightning at Wind Turbines: Risk Assessment from Larger-Scale Meteorology

Isabell Stucke[1,2], Deborah Morgenstern[1,2], Gerhard Diendorfer[3], Georg J. Mayr[2], Hannes Pichler[3], Wolfgang Schulz[3], Thorsten Simon[4], Achim Zeileis[1]

[1]Institute of Statistics, University of Innsbruck, Austria, Innsbruck
[2]Institute of Atmospheric and Cryospheric Sciences, University of Innsbruck, Austria, Innsbruck
[3]OVE Service GmbH, Dept. ALDIS (Austrian Lightning Detection & Information System), Austria, Vienna
[4]Department of Mathematics, University of Innsbruck, Austria, Innsbruck

Key Points:

- Tower-trained random forests can diagnose the risk of upward lightning at wind turbines based on larger-scale meteorological conditions.
- Convective precipitation, larger-scale vertical updraft and the presence of CAPE are most important for upward lightning.
- Slightly elevated terrain and near-coastal conditions tend to increase the risk of upward lightning.

Corresponding author: Isabell Stucke, `isabell.stucke@uibk.ac.at`

Abstract

Upward lightning (UL) has become a major threat to the growing number of wind turbines producing renewable electricity. It can be much more destructive than downward lightning due to the large charge transfer involved in the discharge process. Ground-truth lightning current measurements indicate that less than 50 % of UL could be detected by lightning location systems (LLS). UL is expected to be the dominant lightning type during the cold season. However, current standards for assessing the risk of lightning at wind turbines mainly consider summer lightning, which is derived from LLS. This study assesses the risk of LLS-detectable and LLS-undetectable UL at wind turbines using direct UL measurements at instrumented towers. These are linked to meteorological data using random forests. The meteorological drivers for the absence/occurrence of UL are found from these models. In a second step, the results of the tower-trained models are extended to a larger study area (central and northern Germany). The tower-trained models for LLS-detectable lightning are independently verified at wind turbine sites in this area and found to reliably diagnose this type of UL. Risk maps based on cold season case study events show that high diagnosed probabilities in the study area coincide with actual UL events. This lends credibility to the application of the model to all UL types, increasing both risk and affected areas.

Plain Language Summary

The need to produce renewable energy has recently led to an increase not only in the number of wind turbines, but also in their size. The taller the man-made structure, the greater the likelihood of upward lightning (UL) to initiate from the wind turbine. Each UL event has an initial continuous current, making it ten times longer and much more destructive than a downward lightning event. As UL has become a major weather-related hazard to wind turbines, proper risk assessment has become essential. The problem: Ground-truth current measurements at an instrumented tower in Austria show that less than 50 % of UL is actually detected by lightning location systems (LLS). This study shows that a new approach based on vertically resolved larger-scale meteorology and direct UL measurements from specially instrumented towers, combined with flexible machine learning techniques, succeeds in diagnosing the risk of both LLS-detectable and LLS-undetectable UL at wind turbines in the colder season over a larger study area.

1 Introduction

The growing importance of renewable energy production has recently led to a significant increase in the number of wind turbines (e.g., Pineda et al., 2018). As these structures are typically taller than 100 m, the initiation of upward lightning (UL) propagating from the tall structure towards the clouds is facilitated (Berger, 1967). A tall structure is more likely to experience UL because it is exposed to a stronger electric field compared to the ground. Structures shorter than 100 m mainly experience downward lightning (DL) with leaders propagating from the clouds towards the earth's surface (e.g., Rakov & Uman, 2003).

As wind turbines become taller, UL is the main weather-related cause of severe damage to them (e.g., Rachidi et al., 2008; Montanyà et al., 2016; Pineda et al., 2018; Matsui et al., 2020; Zhang & Zhang, 2020). It can be much more destructive than DL because its initial continuous current (ICC) lasts about ten times longer than the current flow of DL. Ground-truth lightning current measurements on the specially instrumented tower at the top of the Gaisberg mountain (Austria, Salzburg) show that more than 50 % of UL is not detected by conventional lightning location systems (LLS). The reason is that the LLS cannot detect a certain subtype of UL with only an ICC (Diendorfer et al., 2015; March et al., 2016). Although there are towers providing ground-truth lightning current data for LLS-detectable UL (UL-LLS), such as the Säntis Tower in Switzerland, the Gaisberg Tower is the only instrumented tower in Europe providing full information on the occurrence of both UL-LLS and LLS-undetectable UL (UL-noLLS).

Standards for lightning protection of wind turbines (IEC 61400-24, 2019) crucially underestimate the occurrence of UL at wind turbines as they currently rely on only three factors: The height of the wind turbine, the local annual flash density derived from LLS, and an environmental term that includes factors such as terrain complexity or altitude (Rachidi et al., 2008; Pineda et al., 2018; March, 2018; Becerra et al., 2018). Summer lightning activity clearly dominates the annual local flash density due to large amounts of DL caused by deep convection. However, UL is expected to be the dominant lightning type at wind turbines with a tendency to be even more important in the colder season (Diendorfer, 2020; Rachidi et al., 2008). Furthermore, the risk assessment standards cannot take into account UL-noLLS, but only UL-LLS if a tall structure is present.

The main objective of this study is to assess the risk of UL-LLS and UL-noLLS on wind turbines over a larger area. Although LLS are available to analyze UL-LLS at tall structures, direct lightning current measurements show that a significant proportion is missed. Recognizing that conventional LLS cannot assess the full risk of UL at wind turbines, a new approach is used in this study.

It uses machine learning techniques to link the occurrence of UL to the larger-scale meteorological environment. The occurrence of UL can only be provided by ground-truth lightning current measurements. These form the basis for building and training the statistical models that will ultimately be used to assess the risk of UL over an entire study area. Specifically, this study uses conditional inference random forests (Hothorn & Zeileis, 2015), which account for the highly non-linear and complex interactions between the incidence of UL on the tall structures and the atmosphere. Several steps are required to achieve the main goal.

From direct lightning current measurement data at two instrumented towers in Austria (Gaisberg Tower) and Switzerland (Säntis Tower), two models are constructed: One for UL-LLS and one for UL-LLS + UL-noLLS. The aim of these models is, firstly, to determine whether there is a relationship between larger-scale meteorological variables and the occurrence of UL and, secondly, to demonstrate how well larger-scale meteorology can serve as a diagnostic tool for inferring the occurrence of UL.

The advantage of the availability of UL-LLS data helps to verify whether the results from the instrumented towers are transferable. The idea is to extract wind turbine sites within the study area and identify all lightning strikes to them from the colder season (ONDJFMA) using LLS data. Success in reliably diagnosing UL-LLS from larger-scale meteorology in combination with UL ground-truth lightning current measurements provides greater confidence in the results when, in a final step, the risk of UL-noLLS, which cannot be verified using LLS data, is assessed.

The following sections are organized as follows. Section 2 introduces the two instrumented towers that provide the necessary ground-truth data for this study. The first is the Gaisberg Tower, which provides both UL-LLS and UL-noLLS, and the second is the Säntis Tower, which provides only UL-LLS. Furthermore, this section presents the identification of lightning at wind turbines in the study area and the meteorological data used. Section 3 summarizes the procedures and main results from the two instrumented towers. Section 3.1 describes the basic principle of building a random forest model. Section 3.2 presents the performance of the models on the instrumented towers. Furthermore, the most important larger-scale meteorological variables leading to a higher risk of UL are introduced (section 3.3). Then, section 4 presents the results of extending the models from the instrumented towers to the larger study area to find regions with a higher risk of experiencing UL. Section 4.1 diagnoses UL-LLS on wind turbines and presents case studies. Section 4.2 then illustrates and discusses the risk of UL-LLS and UL-LLS

+ UL-noLLS on wind turbines for the entire study period. Section 5 concludes and summarizes the most important findings.

2 Data

This study combines five different data sources: UL data measured directly at the Gaisberg Tower in Austria (Diendorfer et al., 2009) and at the Säntis Tower in Switzerland (Romero et al., 2012); LLS data measured remotely by the European Cooperation for Lightning Detection (EUCLID, Schulz et al., 2016); larger-scale meteorological variables from the reanalysis database ERA5 (Hersbach et al., 2020); wind turbine locations identified using the © OpenStreetMap (OpenStreetMap contributors, 2020) database.

2.1 Direct UL measurements at instrumented towers

Figure 1 shows two of the very few instrumented towers for direct measurement of currents from UL. These are the Gaisberg Tower (1 288 m amsl, 47°48′ N, 13°60′ E) and the Säntis Tower (2 502 m amsl, 47°14′ N, 9°20′ E). Lightning at the instrumented towers is almost exclusively UL. Gaisberg Tower recorded a total of 819 UL events between 2000 and 2015. Säntis Tower recorded 692 UL events between 2010 and 2017.

A sensitive shunt type sensor at Gaisberg allows measurement of all types of upward flashes regardless of the current waveform, that is, UL-LLS and UL-noLLS. However, the inductive sensors used by Säntis cannot measure upward flashes with only an ICC (about 50 %, Diendorfer et al., 2015).

Direct UL current measurements are critical to the construction of the random forest models, which are extended to the larger study area after training on the tower data. The combination of data from both towers provides a sufficiently large dataset and allows the construction of the two types of models to diagnose both UL-LLS and UL-LLS + UL-noLLS.

2.2 UL-LLS at wind turbines and study domain

Remotely detected lightning data from the LLS EUCLID and wind turbine locations derived from © OpenStreetMap serve as verification of the statistical models assessing the risk of UL-LLS for the selected study area.

Within the study area of 50°N–54°N and 6° E–16°E, 27,814 wind turbines have been installed by the end of 2020 (Fig. 1). After extracting the exact locations of these wind turbines, lightning strikes within a 0.003° circular area (approximately within 300 m radius) detected by EUCLID are identified and assumed to be UL. EUCLID measures DL with a high lightning detection efficiency of more than 90 % (Schulz et al., 2016). As mentioned above, UL may be detected less efficiently (< 50 % Diendorfer et al., 2015).

Due to its destructive potential and its severe underestimation in current lightning protection standards, UL, and in particular the risk of UL at wind turbines, shall be explicitly considered in this study. The tower-trained models are based on UL data throughout the year. However, since UL is expected to be dominant in the colder season compared to DL, only the months from October to April, starting from October 2018 to December 2020, are considered in the verification part of the study. Furthermore, since DL is dominant in the warmer season, the extraction of lightning strikes to wind turbines would possibly lead to ambiguity in the identification of DL or UL when considering the whole year.

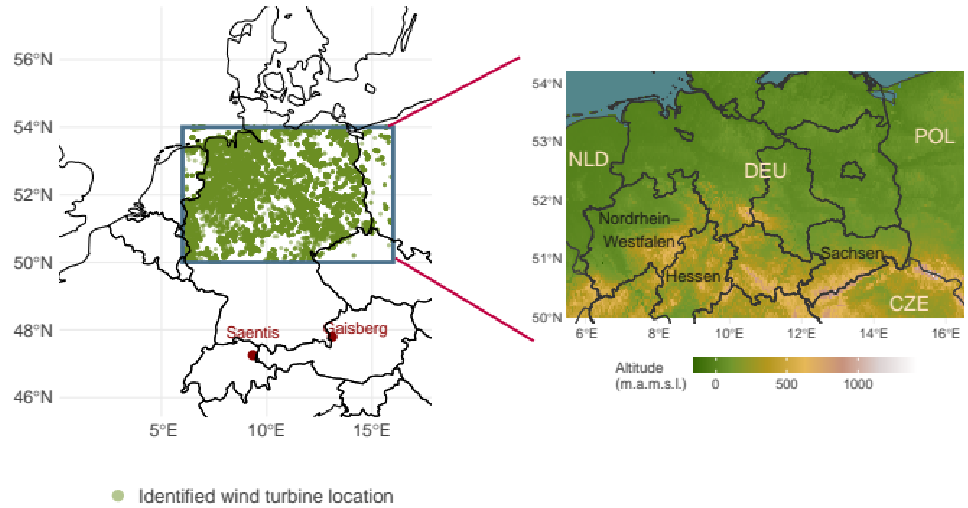

Figure 1. Geographic overview of the instrumented tower locations (Gaisberg and Säntis) as well as the study domain (box). Green dots are manually identified wind turbine locations based on © OpenStreetMap 2020. Right: topographic map of study domain showing altitude above mean sea level. Data taken from Shuttle Radar Topography Mission (Farr & Kobrick, 2000).

2.3 Meteorological data

ERA5 provides an hourly reanalysis of the state of the atmosphere. It has a resolution of 31 km horizontally (grid cell size of 0.25 x 0.25) and 137 levels vertically. This study uses 35 directly available and derived surface, model level, and vertically integrated variables. These reflect variables relevant to cloud electrification, lightning, and thunderstorms (Morgenstern et al., 2022). A complete list of variables can be found in the supporting information file. The data are spatially and temporally bilinearly interpolated to each Gaisberg and Säntis Tower UL observation as well as to each grid cell within the study domain in the verification part of this study.

3 Methodological procedures and findings from the instrumented towers

This section provides the necessary background information on the basic methods as well as important results from the analysis of the instrumented Gaisberg Tower and Säntis Tower. Three different aspects will be covered: First, the principle of how the basic model, a random forest, is constructed and verified. Second, the performance of the models and third, which variables are most important to identify favorable conditions for UL to occur or not.

3.1 Construction and verification of the tower-trained random forests

A machine learning technique that has recently been widely applied in various scientific fields is used to link larger-scale meteorology and the occurrence of UL at the instrumented towers. Random forests Breiman1984 are highly flexible and able to handle nonlinear effects, capturing complex interactions with respect to the stated modeling problem (Strobl et al., 2009).

The occurrence versus non-occurrence of UL is a binary classification problem, which is tackled using 35 larger-scale meteorological variables (predictors). Each meteorological predictor is linked to a situation with or without UL at Gaisberg or Säntis Tower using a random forest. A random forest combines predictions from multiple decision trees trained on randomly selected subsamples of the input data.

Specifically, the trees in the random forest are constructed by capturing the association between the binary response and each of the predictor variables using permutation tests (also known as conditional inference, see Strasser and Weber (1999)). The idea is that at each step in the recursive tree construction, the one predictor variable that has the highest (most significant) association with the response variable is selected. Then, the data set is split with respect to this predictor variable in order to separate the different response classes as well as possible. The splitting is repeated recursively in each of the subsets of the data until some stopping criterion (e.g., regarding significance or subsample size) is met. The forest combines 500 of such trees, where each tree is learned on randomly subsampled two-thirds of the full data set, and only six randomly selected predictors are considered in each split. Finally, the random forest averages the predictions from the ensemble of trees, which stabilizes and improves the prediction performance. See Hothorn et al. (2006) and Hothorn and Zeileis (2015) for more details on the algorithm and implementation.

To validate the resulting models, the input data is split into training and test data samples. The training data is used to train the models, and the unseen test data is used to evaluate the diagnostic capability. Leave-one-out cross-validation is used to validate the models for UL-LLS and UL-LLS + UL-noLLS. The first model for UL-LLS uses both Säntis data and Gaisberg data to increase the size of the training data. The particular flash type that cannot be detected by the Säntis Tower is omitted from the Gaisberg data during training to ensure consistency. The second model for UL-LLS + UL-noLLS uses only Gaisberg data because only the Gaisberg Tower provides complete information on all subtypes of UL.

Between 2000 and 2015, the Gaisberg Tower experienced 247 unique days with UL events. Between 2010 and 2017, the Säntis Tower experienced 186 unique days. Combining the UL days from both towers yields 406 unique days with UL. Each training input data set omits one of the 247 (406) days with UL to use it as test data. This is repeated until each of the 247 (406) days is omitted once for training the random forest models. This results in 247 (406) different models trained on situations with and without UL.

The input model response (that is, did UL occur or not) is sampled so that the two classes are balanced, that is, situations with and without UL are present in equal proportions. To evaluate the performance of the models, the models diagnose the conditional probability on data not considered in the training of the models, that is, on the omitted day. We call the probability conditional because of the balanced model response setup. In order to diagnose the conditional probability of UL also on days without UL, days without UL are randomly sampled from each season between 2000 and 2017. A high diagnostic ability refers to high probabilities when UL occurred at Gaisberg or Säntis in the particular situation (that is, a high true positive rate) and low probabilities when no UL occurred (that is, a low false positive rate).

3.2 Performance of the tower-trained random forests

The tower-trained random forest models can reliably diagnose both UL-LLS and UL-LLS + UL-noLLS when validated on unseen withheld data from the towers. Figure 2 summarizes the cross-validated diagnostic ability according to the random forests for UL-LLS + UL-noLLS (Gaisberg) and UL-LLS (Gaisberg + Säntis). Both model ensembles show similar good diagnostic performance. The diagnosed median conditional prob-

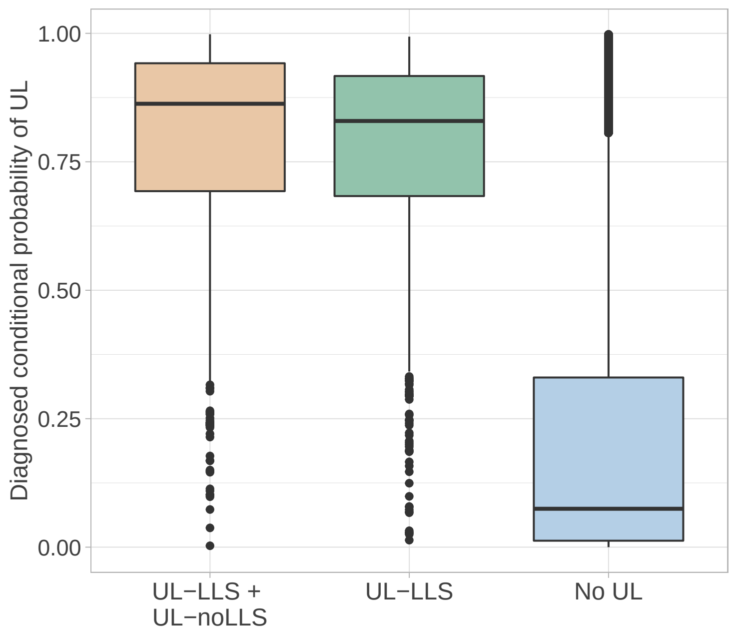

Figure 2. Distributions of diagnosed conditional probabilities in situations with or without UL events. Left: conditional UL probability given that UL was observed in the particular minute (true positive) based on Gaisberg data including all subtypes of UL. Center: conditional UL probability given that UL was observed in the particular minute based on Gaisberg and Säntis data combined. Right: conditional UL probability on randomly sampled days without UL events (false positive).

abilities are about 0.8 that UL was observed in the respective situation (minute). This indicates a high true positive rate. Similarly, for situations without lightning (right), the conditional probabilities are low, indicating a low false positive rate.

The fact that the random forest including UL-noLLS has the highest diagnostic ability shows that the fraction not detected by conventional LLS can indeed be reliably diagnosed by larger-scale meteorology alone. This supports the idea to also investigate the risk of undetectable UL-noLLS and not only UL-LLS.

3.3 Meteorological drivers for UL-LLS at the instrumented towers

Random forests allow to assess the influence of individual variables on the diagnostic performance of the models. This is done by calculating the so-called permutation variable importance. The idea is to break the relationship between the response variable and a predictor variable by neglecting its information when assessing the diagnostic performance of the models. Neglecting the information of a predictor variable is done by permutation, that is, randomly shuffling its values and then assessing how much the diagnostic performance decreases. Figure 3 visualizes the calculated median permutation variable importance according to 100 different random forest models for UL-LLS. Each of the 100 models is based on a balanced proportion of situations with UL and randomly selected situations without UL. The results for the UL-LLS and UL-LLS + UL-noLLS models are very similar.

Convective precipitation has the largest influence on the occurrence of UL according to the random forests based on direct observations from Gaisberg and Säntis Tower (Fig. 3). Neglecting the information of this driver variable reduces the diagnostic performance the most. The second and third most important variables are the maximum updraft velocity and the convective available potential energy (CAPE). A statistical summary of the three most important variables shows that the CAPE at both the Säntis Tower and the Gaisberg Tower is rather low when UL occurs (median value of 68 J kg^{-1}). Convective precipitation comes with a median of 3.8 mm and maximum vertical updraft velocity with a median of $-$ 1.5 m s^{-1}. All values are larger in magnitude than the "average" when looking at every single hour in the time range considered. However, the order of magnitude is not exceptionally high, as can be observed for deep convection, where especially the CAPE values are often higher than 500 J kg^{-1}. An important reason for this may be that at the instrumented towers, UL occurs approximately evenly throughout the year, whereas intense thunderstorms with deep convection and high CAPE values occur mainly in the summer season. Further, this may suggest that the occurrence of UL requires a combination of many different processes that interact to create favorable conditions for UL, which may be even more complex than creating favorable conditions for deep convection.

Other important variables are the maximum precipitation rate, the vertical size of the thundercloud, the amount of ice crystals and solid hydrometeors, and the 2 m dew point temperature.

4 UL at wind turbines

Extraction of wind turbine locations and identification of lightning strikes to them within 300 m in the cold season (ONDJFMA) shows that there are regions within the study area that experience UL more frequently than others (see Fig. 4). Interestingly, the regions that experience UL more frequently (panel (b), dark pink) coincide with regions with many wind turbines. In general, however, it can be observed that regions with a high number of wind turbines (panel (a), dark green) do not necessarily coincide with a high number of ULs, as can be seen for example in the northeastern parts of the study area. The following sections present and discuss the results of extending the results from

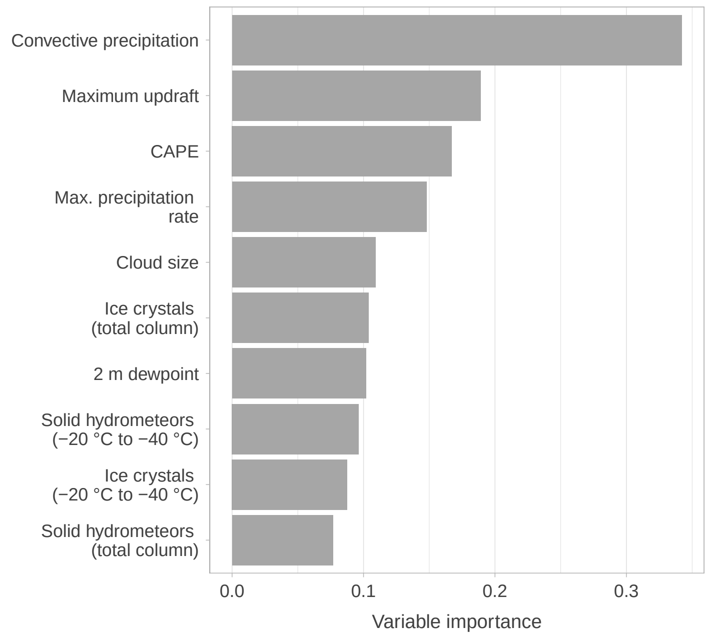

Figure 3. Median permutation variable importance according to 100 different random forests based on balanced proportions of situations with and without UL at the Gaisberg and Säntis Tower.

the instrumented towers to the study area by extracting the locations of wind turbines and analyzing the lightning activity to them.

4.1 Diagnosing UL-LLS at wind turbines from larger-scale meteorological conditions

The random forest models for UL-LLS and UL-LLS + UL-noLLS, based on data from the two instrumented towers, identified larger-scale meteorological variables that are the most important discriminators between situations with and without UL. The tower-trained random forest models are now applied to the larger study area to assess the risk of UL at wind turbines. Lightning measurements from LLS data will verify the results at identified wind turbine sites.

The following results are based on a similar procedure as described in Sect. 3.2, except that each grid cell (31 km x 31 km) of the study domain is used as test data instead of the cross-validated data from the instrumented towers.

To increase the robustness of the results, again 100 different random forest models based on observations from the Gaisberg and the Säntis Tower are used to diagnose the conditional probability of UL on the selected case studies over the study domain. The results in this section visualize the median conditional probabilities diagnosed by the random forest models.

Case studies: UL-LLS at wind turbines

To illustrate the diagnostic ability of the tower-trained random forests for UL-LLS on days with UL events, three different case study days are selected from the colder seasons between 2018 and 2020 in the study area.

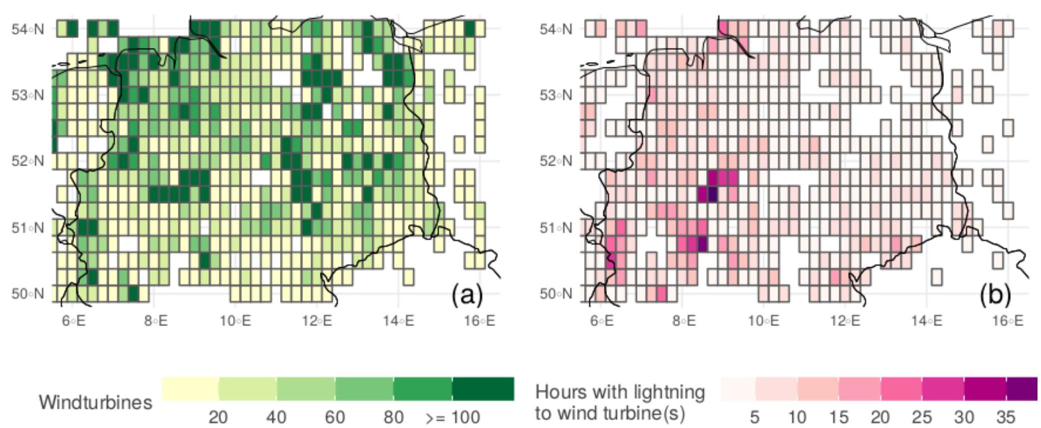

Figure 4. Panel (a): number of wind turbines per grid cell derived from © OpenStreetMap 2020 data. Panel (b): number of hours per grid cell with lightning at wind turbines derived from EUCLID data.

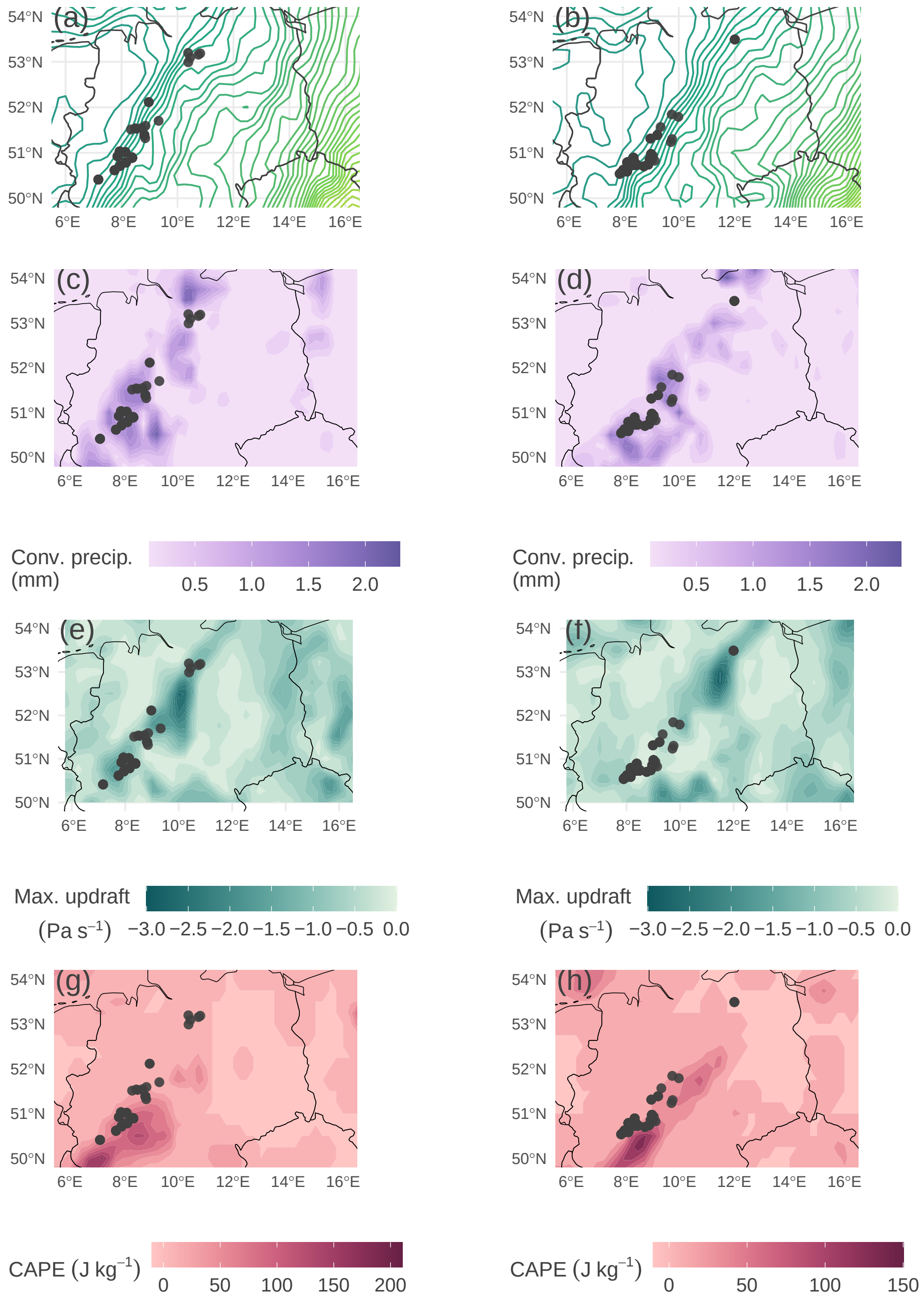

Figure 5. Larger-scale meteorological setting on the $4th$ March 2019 over the study domain. Left column illustrates the setting at 13 UTC, right column at 14 UTC. From upper to lower: spatial distributions of isolines of the 850 hPa temperature (in intervals of 1 K), convective precipitation, the maximum large-scale updraft velocity (negative values is upward motion) and CAPE. Darker colors indicates higher magnitude. Dark gray dots in all figures are flashes within the considered hour and ERA5 grid cell derived from LLS EUCLID data.

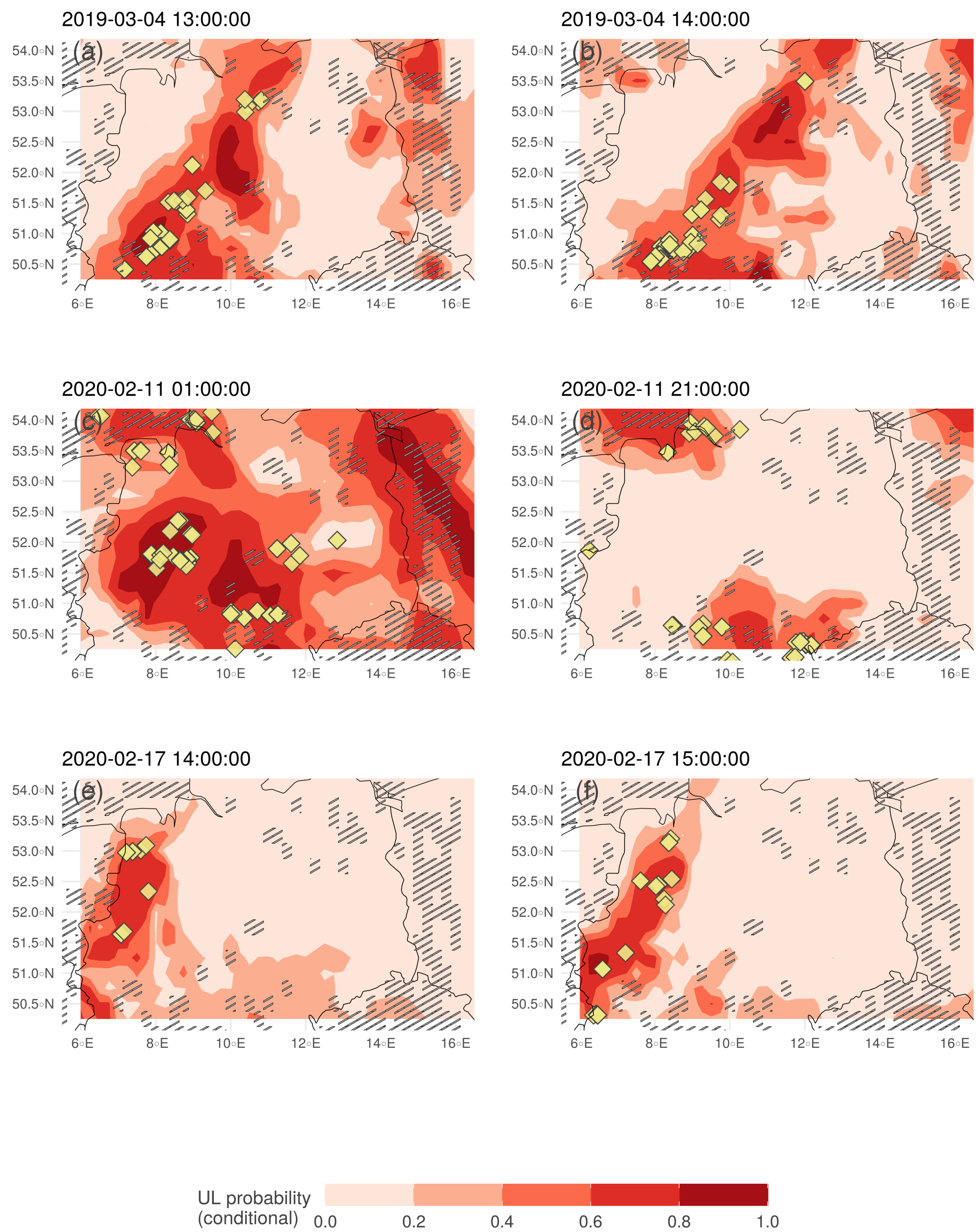

Figure 6. Median diagnosed conditional probability of UL according to 100 random forest models based on Gaisberg and Säntis Tower data (red areas). Yellow symbols are flashes within the considered hour derived from EUCLID data. Gray shaded areas are grid cells without wind turbines.

The selected case study days are characterized by typical weather situations for the colder seasons in the mid-latitudes. The atmosphere in the transitional seasons and in winter tends to be highly variable and influenced by the succession of cyclones and anticyclones that determine the meteorological setting (Perry, 1987). In particular, the development and progression of mid-latitude cyclones provide favorable conditions for so-called wind field thunderstorms (Morgenstern et al., 2022). This type of thunderstorm is associated with, among other things, strong updrafts, high precipitation amounts, and low but present CAPE.

The first case study is considered in more detail with respect to the drivers identified at the instrumented towers (Fig. 3). Figure 5 illustrates the larger-scale isotherm locations, spatial distribution of convective precipitation, maximum updraft velocity, and CAPE on 4 March 2019 at 13 UTC and 14 UTC. LLS detected lightning events at the identified wind turbines within the respective hour are indicated as dark gray dots.

The meteorological setting is determined by the passage of a cold front ahead of a trough around noon. Densely packed isotherms at 850 hPa crossing northern and central Germany from west to east indicate the approximate location of the cold front in panels (a) and (b). The cold front implies locally increased amounts of convective precipitation in (c) and (d), strong updrafts indicated by large negative values in (e) and (f), and slightly increased but generally low CAPE in (g) and (h) compared to deep convection in summer. All three variables show maximally increased values in slightly different areas within the study area induced by the cold front. Convective precipitation shows increased values along the cold front, while the other two variables have locally more concentrated areas with maximum values (e.g. maximum updraft velocity in North/Central Germany).

Figure 6 visualizes the diagnosed conditional probability by the random forest models in red colors for all three case study days. Panels (a) and (b) show the results for the particular case study discussed in Fig. 5. The diagnosed pattern is a result of combining the influence of the three driver variables. This suggests that no single variable can be responsible for the resulting probability map, but rather an interaction of different influencing variables resulting in areas of increased risk of experiencing UL.

The yellow symbols again show lightning strikes over the hour considered. Identified lightning events in yellow require a wind turbine within a maximum distance of 300 m as described in Sect. 2. All other tall structures that may have experienced UL are not considered in this figure. Since the diagnosed probabilities do not depend on wind turbine locations, high probabilities may be diagnosed even though there is no wind turbine installed. Grid cells without wind turbines are shaded gray.

All three case study days in Fig. 6 show that areas with increased diagnosed probability of UL coincide well with identified lightning events in that hour over the study area. In all three case studies, there is a clear separation between areas with very low diagnosed risk and areas with very high diagnosed risk of experiencing UL.

On 11 February 2020, shown in panels (c) and (d) of Fig. 6, the study domain is again in a strong westerly flow associated with locally enhanced convective precipitation, CAPE, and strong updrafts (not shown here). On February 17, 2020, the study area is crossed by a cold front at higher altitudes (above 500 hPa). Despite the different meteorological situation, the conditions are similar to the other case studies, showing elevated values in the three driver variables that strongly influence the diagnosed conditional probability.

4.2 Risk assessment of UL at wind turbines

Identifying areas of increased UL risk due to larger-scale meteorological conditions is a valuable step in assessing the risk of lightning at wind turbines. The case studies clearly show that the observed lightning events at wind turbines coincide with the areas of increased probability diagnosed by the random forest models. The following analysis considers all events within the considered time period in which lightning was detected at wind turbines. Not only the models for UL-LLS shall provide a risk assessment, but now the random forests for UL-LLS + UL-noLLS are additionally applied to the study area and the considered time period.

The considered study period including the transition seasons and winter from 2018 to 2020 counts a total of 185 event days with 1 027 single flash hours and 18 602 single flash events. These numbers are intended as a measure to verify the resulting diagnostic probabilities from the random forest models. Note that these numbers are the lower bound of the number of flashes that actually occurred. Taking into account the uncertainty of manual identification of flashes at wind turbines as well as the uncertainty of UL detection by the LLS, a significantly higher number of actual lightning events at wind turbines can be expected. Furthermore, this verification approach only considers lightning at wind turbines and neglects all other tall structures such as radio towers in the study area that could be affected by UL. In the following, all days within the considered study period are taken as new data for the random forest models to diagnose the conditional probabilities on an hourly basis.

The goal is to identify regions that, according to the random forest models, have a higher risk of UL compared to other regions. This is done by counting the number of hours in each ERA5 grid cell (0.25 x 0.25) that exceed the conditional probability threshold of 0.5.

Risk assessment of UL-LLS at wind turbines

Figure 7a illustrates that there are regions in the study area that have a higher risk of experiencing UL-LLS more frequently than other regions. The western and southwestern parts of the study area have a significantly higher probability of UL-LLS. This is also consistent with panel (b) in Fig. 4, which shows the actually observed hours in which at least one lightning event occurred to a wind turbine within the respective grid cell. Interestingly, areas with higher UL-LLS probabilities in Fig. 7 roughly coincide with regions of elevated topography in the southern third of the domain (cf. Fig. 1). Possible explanations are an increased lightning-effective height (e.g., Shindo, 2018) of the turbines and increased chances for thunderstorm formation due to orographic uplift and thermally induced breezes (Kirshbaum et al., 2018). Sea breezes may also explain the higher probabilities in the northwesternmost, ocean-covered part of the domain.

The successful transfer of the UL-LLS model trained with meteorological data from direct tower measurements to a larger region and its independent verification on wind turbines shows the potential of our approach to produce regionally varying risk maps, which in turn could lead to regionally varying (voluntary or enforced) lightning protection standards for wind turbines.

Risk assessment of UL-LLS + UL-noLLS at wind turbines

The successful transfer of the tower-trained and verified UL-LLS model to a larger domain lends credence to taking the same step with the tower-trained model for all upward lightning (UL-LLS and UL-noLLS), although no data are available for independent verification.

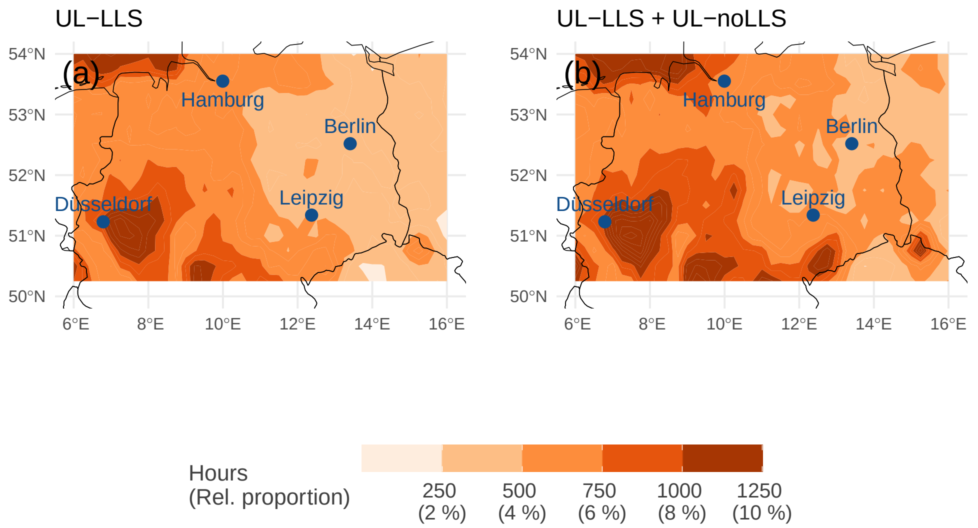

Figure 7. Panels (a) and (b): potential maps for UL in the colder season (ONDJFMA) from 2018 to 2020. Orange colors are median of hours per grid cell exceeding conditional probabilities of 0.5 according to 100 random forest models. Panel (a) shows results according to models based on Gaisberg and Säntis data combined. Panel (b) shows results according to models based on Gaisberg data also including the UL-noLLS. Relative proportion of in total 12480 hours are given as reference.

Panel (b) in Fig. 7 shows that more flashes are expected when the LLS-undetectable UL flash type is added. The pattern of areas with increased risk of experiencing UL is similar, although some of the more frequently affected areas are enlarged. This suggests that there are similar mechanisms resulting from larger-scale meteorology that lead to the UL-LLS or UL-noLLS flash types. The risk is most pronounced in regions with elevated topography in the southern part of the domain and in the northwesternmost coastal region.

5 Conclusions

Upward (UL) lightning that strikes tall structures such as wind turbines is much more destructive than downward (DL) lightning. Each UL flash begins with an initial continuous current (ICC) that lasts about ten times longer than DL, transferring much more charge to the tall structure. Furthermore, direct measurements of upward lightning suggest that less than 50 % of UL events can be detected by most lightning location systems (LLS) because they are unable to detect UL with only an ICC.

Current lightning protection standards are based on the annual flash density derived from LLS data, which is clearly dominated by DL in the warm season. UL that is not detectable by LLS (UL-noLLS) is completely neglected and UL in the cold season is severely underestimated. The basic knowledge about the occurrence of UL is still incomplete, which hinders a proper risk assessment of UL at wind turbines.

The lack of consideration of UL-noLLS and the importance of the cold season for UL will therefore significantly underestimate the risk of UL to wind turbines. This study uses rare direct UL measurements with larger-scale meteorological data in a machine learning model to estimate the risk of all UL, including UL-noLLS, on wind turbines.

This study's first step is to train and validate two different random forest models based on long-term observations from two specially instrumented towers. One model considers only LLS-detectable UL (UL-LLS) and one model considers UL-LLS + UL-noLLS. The model input data are direct UL measurements from the Gaisberg Tower (Austria, 2000-2015) and the Säntis Tower (Switzerland, 2010-2017). While the sensor at the Gaisberg Tower also measures UL-noLLS, the sensor at the Säntis Tower misses most of them.

In a second step, the random forest models are extended to a larger study area (50°N–54°N and 6° E–16°E) to identify areas with increased risk of UL in the colder season (ONDJFMA). As a verification, all lightning strikes from LLS data on wind turbines extracted from © OpenStreetMap data are compared to the diagnosed probabilities by the random forests.

The results show that UL can be reliably diagnosed by the tower-trained random forest models at the Gaisberg and Säntis towers. The larger-scale meteorological drivers are large amounts of (convective) precipitation, strong vertical updraft velocities, and slightly elevated CAPE. Furthermore, the vertical extent of the clouds and the amount of ice crystals and solid hydrometeors are important variables.

Extending the random forests to a larger domain shows that the probability maps match the observed lightning strikes at wind turbines. The extension of the models trained at the Gaisberg Tower to include UL-noLLS flashes shows that areas with an increased risk of experiencing UL are expected to experience UL even more frequently. The western and southern part of the domain in northwestern Germany with elevated topography and the coastal region in the northwesternmost part are most at risk for UL at wind turbines.

This study demonstrates that direct UL measurements at an instrumented tower can be reliably modeled from larger-scale meteorological conditions in a machine learning model (random forest). The study also proposes a novel way to justify the transfer of this model to a larger region using UL-LLS data at wind turbine sites. As a result, regionally detailed risk maps of UL at wind turbines can be produced.

Open Research

Data availability

ERA5 data are freely available at the Copernicus Climate Change Service (C3S) Climate Data Store Hersbach et al. (2020). The results contain modified Copernicus Climate Change Service information (2020). Neither the European Commission nor ECMWF is responsible any use that may be made of the Copernicus information or data it contains. EUCLID data and ground truth lightning current measurements from the Gaisberg Tower are available only on request. For more details contact Wolfgang Schulz or Siemens BLIDS.

Software

All calculations as well as setting up the final data sets, modeling and the diagnosis were performed using R R Core Team (2021), using packages netCDF4 Pierce (2019), partykit Hothorn and Zeileis (2015), ggplot2 package Wickham (2016). Retrieving the raw data and deriving further variables from ERA5 required using Python3 Van Rossum and Drake (2009) and cdo Schulzweida (2019).

Competing interests

The authors declare that they have no conflict of interest.

Acknowledgements

We acknowledge the funding of this work by the Austrian Research Promotion Agency (FFG), project no. 872656 and Austrian Science Fund (FWF) grant no. P 31836. We thank the EMC Group of the Swiss Federal Institute of Technology (EPFL) for providing the data of the Säntis Tower strikes.

Provided Author contributions

Isabell Stucke: Conceptualization, Data Curation, Formal Analysis, Investigation, Methodology, Validation, Software, Visualization, Writing – Original Draft, Writing – Review Editing, Deborah Morgenstern: Conceptualization, Data Curation, Writing – Review Editing, Gerhard Diendorfer: Conceptualization, Funding Acquisition, Resources, Writing – Review Editing, Georg J. Mayr: Conceptualization, Funding Acquisition, Project Administration, Supervision, Writing – Review Editing , Hannes Pichler: Conceptualization, Funding Acquisition, Resources, Wolfgang Schulz: Conceptualization, Funding Acquisition, Resources, Writing – Review Editing , Thorsten Simon: Conceptualization, Data Curation, Formal Analysis, Supervision, Writing – Review Editing , Achim Zeileis: Formal Analysis, Methodology, Project Administration, Software, Supervision, Writing – Review Editing

References

Becerra, M., Long, M., Schulz, W., & Thottappillil, R. (2018). On the estimation of the lightning incidence to offshore wind farms. *Electric Power Systems Research*, *157*, 211–226. Retrieved from `https://www.sciencedirect.com/science/article/pii/S0378779617304790` (accessed 2022-12-22) doi: 10.1016/j.epsr.2017.12.008

Berger, K. (1967). Novel observations on lightning discharges: Results of research on mount san salvatore. *Journal of the Franklin Institute*, *283*(6), 478–525. Retrieved from `https://www.sciencedirect.com/science/article/pii/0016003267905984` (accessed 2023-03-08) doi: 10.1016/0016-0032(67)90598-4

Diendorfer, G. (2020). *Probability of lightning strikes to wind turbines in europe during winter months* (Tech. Rep.). Copernicus Meetings. doi: 10.5194/egusphere-egu2020-3337

Diendorfer, G., Pichler, H., & Mair, M. (2009). Some parameters of negative upward-initiated lightning to the gaisberg tower (2000–2007). *IEEE Transactions on Electromagnetic Compatibility*, *51*(3), 443–452. Retrieved from https://ieeexplore.ieee.org/document/5089467 (accessed 2021-05-24) doi: 10.1109/TEMC.2009.2021616

Diendorfer, G., Pichler, H., & Schulz, W. (2015). LLS detection of upward initiated lightning flashes. In *Proc. 9th asia-pacific international conference on lightning (APL)* (p. 5). Nagoya, Japan. Retrieved from https://www.ove.at/fileadmin/user_upload/aldis/publication/2015/2_APL2015_Diendorfer.pdf (accessed 2021-06-17)

Farr, T. G., & Kobrick, M. (2000). Shuttle radar topography mission produces a wealth of data. *Eos, Transactions American Geophysical Union*, *81*(48), 583–585.

Hersbach, H., Bell, B., Berrisford, P., Hirahara, S., Horányi, A., Muñoz-Sabater, J., … Thépaut, J.-N. (2020). The ERA5 global reanalysis. *Quarterly Journal of the Royal Meteorological Society*, *146*(730), 1999–2049. Retrieved from https://rmets.onlinelibrary.wiley.com/doi/abs/10.1002/qj.3803 (accessed 2021-04-12) doi: 10.1002/qj.3803

Hothorn, T., Hornik, K., & Zeileis, A. (2006). Unbiased recursive partitioning: A conditional inference framework. *Journal of Computational and Graphical Statistics*, *15*(3), 651–674. (accessed 2022-04-27) doi: 10.1198/106186006X133933

Hothorn, T., & Zeileis, A. (2015). partykit: A modular toolkit for recursive partytioning in R. *Journal of Machine Learning Research*, *16*(118), 63905–3909. Retrieved from http://jmlr.org/papers/v16/hothorn15a.html (accessed 2022-04-27)

IEC 61400-24. (2019). *International standard: Wind energy generation systems - part 24: Lightning protection* (Second ed.). Geneva, Switzerland: International Electrotechnical Commission (IEC).

Kirshbaum, D., Adler, B., Kalthoff, N., Barthlott, C., & Serafin, S. (2018). Moist orographic convection: Physical mechanisms and links to surface-exchange processes. *Atmosphere*, *9*(3), 80. doi: 10.3390/atmos9030080

March, V. (2018). Key issues to define a method of lightning risk assessment for wind farms. *Electric Power Systems Research*, *159*, 50-57. Retrieved from https://www.sciencedirect.com/science/article/pii/S0378779617303450 (Recent Developments on Lightning Research and Protection Technologies) doi: 10.1016/j.epsr.2017.08.020

March, V., Montanyà, J., Fabró, F., van der Velde Oscar, Romero, D., Solà, G., … Pineda, N. (2016). Winter lightning activity in specific global regions and implications to wind turbines and tall structures. In *2016 33rd international conference on lightning protection (ICLP), 25–30 september 2016, estoril, portugal.* (accessed 2022-04-09) doi: 10.1109/ICLP.2016.7791447

Matsui, M., Michishita, K., & Yokoyama, S. (2020). Cloud-to-ground lightning flash density and the number of lightning flashes hitting wind turbines in japan. *Electric Power Systems Research*, *181*, 106066. Retrieved from https://www.sciencedirect.com/science/article/pii/S0378779619303852?via\%3Dihub (accessed 2021-03-24) doi: 10.1016/j.epsr.2019.106066

Montanyà, J., Fabró, F., van der Velde, O., March, V., Williams, E. R., Pineda, N., … Freijo, M. (2016). Global distribution of winter lightning: A threat to wind turbines and aircraft. *Natural Hazards and Earth System Sciences*, *16*(6), 1465–1472. Retrieved from https://www.nat-hazards-earth-syst-sci.net/

16/1465/2016/nhess-16-1465-2016.pdf (accessed 2020-02-19) doi: 10.5194/nhess-16-1465-2016

Morgenstern, D., Stucke, I., Simon, T., Mayr, G. J., & Zeileis, A. (2022). Differentiating lightning in winter and summer with characteristics of the wind field and mass field. *Weather and Climate Dynamics*, *3*(1), 361–375. Retrieved from https://wcd.copernicus.org/articles/3/361/2022/ (accessed 2022-04-07) doi: 10.5194/wcd-3-361-2022

OpenStreetMap contributors. (2020). *Planet dump retrieved from https://planet.osm.org* . https://www.openstreetmap.org.

Perry, A. (1987). Middle latitude climates. In *Climatology* (pp. 581–583). Boston, MA: Springer US. doi: 10.1007/0-387-30749-4_116

Pierce, D. (2019). ncdf4: Interface to unidata netCDF (version 4 or earlier) format data files [Computer software manual]. Retrieved from https://CRAN.R-project.org/package=ncdf4 (R package version 1.17)

Pineda, N., Montanyà, J., Salvador, A., van der Velde, O. A., & López, J. A. (2018). Thunderstorm characteristics favouring downward and upward lightning to wind turbines. *Atmospheric Research*, *214*, 46-63. doi: https://doi.org/10.1016/j.atmosres.2018.07.012

R Core Team. (2021). R: A language and environment for statistical computing [Computer software manual]. Vienna, Austria. Retrieved from https://www.R-project.org/

Rachidi, F., Rubinstein, M., Montanyà, J., Bermudez, J.-L., Sola, R. R., Solà, G., & Korovkin, N. (2008). A review of current issues in lightning protection of new-generation wind-turbine blades. *IEEE Transactions on Industrial Electronics*, *55*(6), 2489–2496. (accessed 2022-04-27) doi: 10.1109/TIE.2007.896443

Rakov, V. A., & Uman, M. A. (2003). *Lightning: Physics and effects.* Cambridge University Press. doi: 10.1017/CBO9781107340886

Romero, C., Paolone, M., Rubinstein, M., Rachidi, F., Rubinstein, A., Diendorfer, G., … Zweiacker, P. (2012). A system for the measurements of lightning currents at the säntis tower. *Electric Power Systems Research*, *82*(1), 34–43. (accessed 2022-04-27) doi: https://doi.org/10.1016/j.epsr.2011.08.011

Schulz, W., Diendorfer, G., Pedeboy, S., & Poelman, D. R. (2016). The european lightning location system EUCLID - part 1: Performance analysis and validation. *Natural Hazards and Earth System Sciences*, *16*(2), 595–605. Retrieved from https://pdfs.semanticscholar.org/dba9/b99d6050e3032b823dc88302fd922b89ab83.pdf (accessed 2020-02-19) doi: 10.5194/nhess-16-595-2016

Schulzweida, U. (2019). *CDO user guide.* doi: 10.5281/zenodo.3539275

Shindo, T. (2018). Lightning striking characteristics to tall structures. *IEEJ Transactions on Electrical and Electronic Engineering*, *13*(7), 938–947. doi: 10.1002/tee.22649

Strasser, H., & Weber, C. (1999). *On the asymptotic theory of permutation statistics* (Report Series SFB "Adaptive Information Systems and Modelling in Economics and Management Science" No. 27). SFB Adaptive Information Systems and Modelling in Economics and Management Science, WU Vienna University of Economics and Business. Retrieved from https://epub.wu.ac.at/102/ (accessed 2023-03-29)

Strobl, C., Malley, J., & Tutz, G. (2009). An introduction to recursive partitioning: Rationale, application, and characteristics of classification and regression trees, bagging, and random forests. *Psychological Methods*, *14*(4), 323–348. (accessed 2022-04-27) doi: 10.1037/a0016973

Van Rossum, G., & Drake, F. L. (2009). *Python 3 reference manual.* Scotts Valley, CA: CreateSpace Independent Publishing Platform. (accessed 2021-03-09)

Wickham, H. (2016). *ggplot2: Elegant graphics for data analysis.* Springer Verlag New York. Retrieved from https://ggplot2.tidyverse.org

Zhang, Y., & Zhang, X. (2020). Statistic analysis of lightning transients on wind turbines. *Journal of Renewable and Sustainable Energy*, *12*(6), 063302. doi: 10.1063/5.0031506

Supporting Information for "Upward lightning at wind turbines: Risk assessment from larger-scale meteorology"

Isabell Stucke[1,2], Deborah Morgenstern[1,2],Gerhard Diendorfer[3], Georg J. Mayr[2], Hannes Pichler[3], Wolfgang Schulz[3], Thorsten Simon[4], Achim Zeileis[1]

[1]Institute of Statistics, University of Innsbruck, Austria, Innsbruck

[2]Institute of Atmospheric and Cryospheric Sciences, University of Innsbruck, Austria, Innsbruck

[3]OVE Service GmbH, Dept. ALDIS (Austrian Lightning Detection & Information System), Austria, Vienna

[4]Department of Mathematics, University of Innsbruck, Austria, Innsbruck

Contents of this file

Introduction This supporting information file consists of three parts: one text section, one figure and one table. The text section describes an additional analysis using a different threshold to define regions with increased risk of UL at wind turbines. The figure shows

---

Corresponding author: I. Stucke, Institute of Statistics University of Innsbruck, Innsbruck, Universitätsstrasse 15, 6020, Austria. (isabell.stucke@uibk.ac.at)

the results on this additional analysis. The table lists the larger-scale meteorological variables used in this study. These are directly taken or derived from the ERA5 database.

0.1. Risk assessment of UL at wind turbines using a higher probability threshold

In Sect. 4.2 the model results for the risk assessment of UL-LLS and UL-LLS + UL-noLLS are presented in the way that hours are counted exceeding a conditional probability of 0.5. Figure S1 illustrates the risk assessment using a higher probability threshold, namely 0.8. The number of hours exceeding this threshold is lower by about a factor of two in comparison to a probability threshold of 0.5. However, the regional pattern is still similar with maxima West/South-West of the study domain.

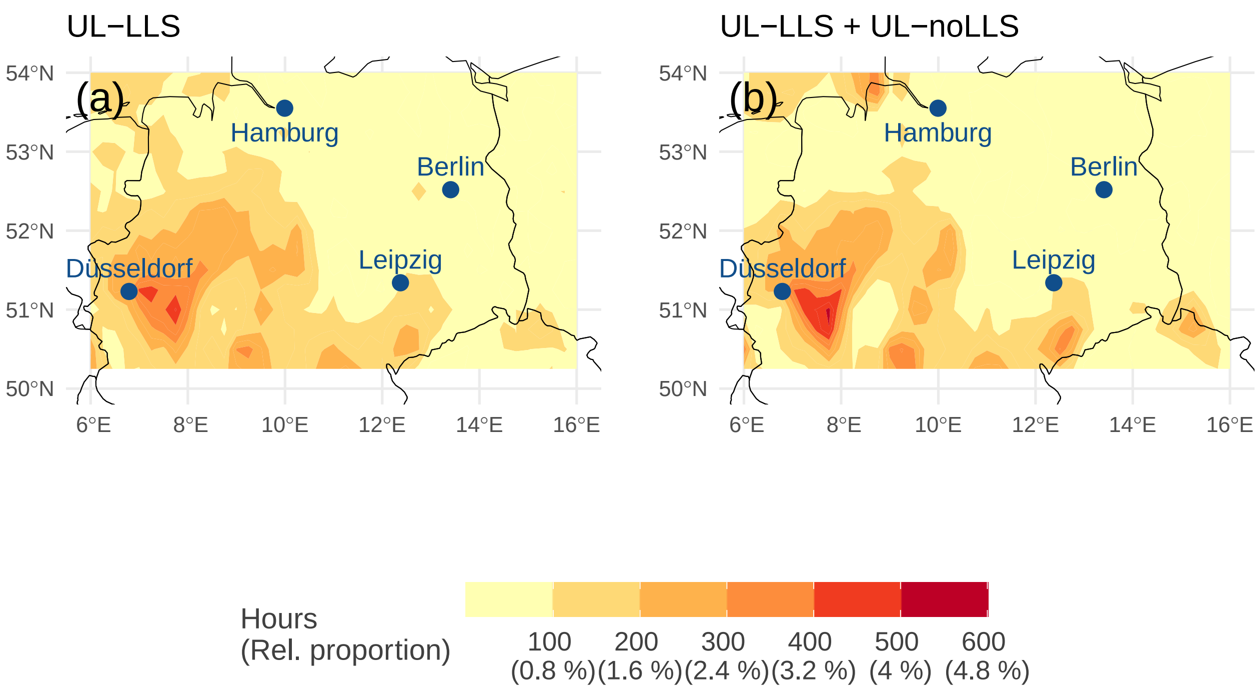

Figure S1. Panels (a) and (b): maps for the potential of UL in the colder season (OND-JFMA) from 2018 to 2020. Orange colors are median of hours per grid cell exceeding conditional probabilities of 0.8 according to 100 random forest models. Panel (a) shows results according to models based on Gaisberg and Säntis data combined. Panel (b) shows results according to models based on Gaisberg data also including the UL-noLLS. Relative proportions of in total 12480 hours are given as reference.

Table S1. Table of large-scale variables taken from ERA5 and variables derived from ERA5. The derived variables (indicated in italics) are suggested to be potentially important in the charging process of a thundercloud or for the development of convection.

Large-scale variables	**Unit**
cloud base height above ground	m agl
convective precipitation (rain + snow)	m
large scale precipitation	m
cloud size	m
maximum precipitation rate (rain + snow)	kg m^{-2} s^{-1}
ice crystals (total column, tciw)	kg m^{-2}
Solid hydrometeors (total column, tcsw)	kg m^{-2}
supercooled liquid water (total column, tcslw)	kg m^{-2}
water vapor (total column)	kg m^{-2}
vertical integral of divergence of cloud frozen water flux	kg m^{-2} s^{-1}
vertical transport of liquids around -10 C	kg Pa s^{-1}
ice crystals (-10 C - -20 C)	kg m^{-2}
ice crystals (-20 C - -40 C)	kg m^{-2}

cloud water droplets (−10 C - −20 C)	kg m^{-2}
solid hydrometeors (−10 C - −20 C)	kg m^{-2}
solid hydrometeors (−20 C - −40 C)	kg m^{-2}
solids (cswc + ciwc) around −10 C	kg m^{-2}
liquids (clwc + crwc) around −10 C	kg m^{-2}
2 m dew point temperature	K
mean vertically integrated moisture convergence	kg m^{-2} s^{-1}
water vapor (−10 C - −20 C)	kg m^{-2}
boundary layer height	m
surface latent heat flux	J m^{-2}
surface sensible heat flux	J m^{-2}
downward surface solar radiation	J m^{-2}
convective available potential energy	J kg^{-1}
convective inhibition present	binary
mean sea level pressure	Pa
height of −10 C isotherm	m agl
boundary layer dissipation	J m^{-2}

Maximum vertical updraft velocity	Pa s^{-1}
total cloud shear	m s^{-1}
wind speed at 10 m	m s^{-1}
wind direction at 10 m	$^\circ$
shear between 10 m and cloud base	m s^{-1}